Universidade de Aveiro
2021

Elena Cassin

Impact of haloazolisin production in the antiarchaeal activity of *Haloferax mediterranei*

Impacto da produção de haloazolisinas na atividade anti-archaea de *Haloferax mediterranei*

Universidade de Aveiro
2021

Elena Cassin

Impact of haloazolisin production in the antiarchaeal activity of *Haloferax mediterranei*

Impacto da produção de haloazolisinas na atividade anti-archaea de *Haloferax mediterranei*

Dissertação apresentada à Universidade de Aveiro para cumprimento dos requisitos necessários à obtenção do grau de Mestre em Biologia Molecular e Celular, realizada sob a orientação científica da Doutora Tânia Caetano, Investigadora Auxiliar do Departamento de Biologia e da Professora Doutora Sónia Mendo, Professora Auxiliar com Agregação do Departamento de Biologia da Universidade de Aveiro.

Dedico este trabalho à minha família e namorado pelo enorme apoio.

o júri

presidente	Prof. Doutor Artur Jorge da Costa Peixoto Alves professor auxiliar com agregação do Departamento de Biologia da Universidade de Aveiro
arguente principal	Prof. Doutora Ana Sofia Direito dos Santos Duarte professora auxiliar da Faculdade de Medicina Dentária da Universidade Católica Portuguesa
orientador	Doutora Tânia Isabel Sousa Caetano investigadora equiparada a auxiliar do Departamento de Biologia e CESAM da Universidade de Aveiro

agradecimentos

Agradeço todas as pessoas que me apoiaram nesse caminho, em particular a minha família, que mesmo longe esteve sempre perto de mim, e o meu namorado. Um agradecimento especial vai a todas as “meninas” do LBM que estiveram ao meu lado todos os dias, a Diana, a Joana e as minhas orientadoras, a Doutora Tânia pelo incansável apoio e continuo estímulo intelectual e a Professora Doutora Sónia pela oportunidade de fazer parte do seu laboratório e desta família.

palavras-chave RiPPs, metabolitos secundário, TOMMs, YcaO

resumo

Halobacteria, também conhecidas por haloarchaea, é uma classe de Archaea halófilas que habitam ambientes. À semelhança de todos os extremófilos, as haloarchaea desenvolveram mecanismos que lhes permitem sobreviver em condições de elevada salinidade, falta de nutrientes e exposição excessiva aos raios UV. Algumas destas adaptações resultam na produção de um conjunto único de metabolitos secundários, tais como carotenóides, sideróforos, poli-hidroxialcanoatos, haloarqueocinas e péptidos ribossomais com modificações pós-traducionais (RiPPs). Os RiPPs de bactérias têm sido amplamente investigados devido à sua diversidade estrutural e bioactividades exibidas, tais como, antibióticos, antivirais e compostos morfogenéticos, entre outros. Contudo, pouco se sabe sobre estes péptidos no domínio Archaea. Recentemente, a análise bioinformática genoma de várias haloarchaea revelou a presença de um grupo de *clusters* biossintéticos (BGCs), designados haloazolinas, que possivelmente codificam para a produção de RiPPs. Nenhum destes BGCs foi investigado experimentalmente, mas todos codificam uma ciclodehydratase pertencente à superfamília YcaO, responsáveis pela instalação de heterociclos de tiazol e oxazol nos péptidos percursores. *Haloferax mediterranei* ATCC 33500 é uma haloarchaea que inibe outras haloarchaea e possui um BGC de haloazolisina constituído, pelo menos, pelo gene da ciclodehidratase (*ycaO*) e pelo péptido percursor (*haloA*). O principal objetivo deste trabalho foi investigar se este BGC está envolvido na actividade anti- haloarchaea de *H. mediterranei*. O crescimento de *H. mediterranei* e a sua bioactividade foi caracterizado ao longo de cinco dias em meio YPC agarizado e concluiu-se que a actividade máxima foi atingida após quatro dias. Por RT-qPCR verificou-se que os genes *ycaO* e *haloA* são transcritos nesta fase do crescimento, embora em níveis diferentes. Foram obtidos dois mutantes de *H. mediterranei* (Δ*ycaO* e Δ*haloA)* aplicando a técnica *popin*/*pop-out*. A eliminação dos genes não influenciou a produção de biomassa e os mutantes mantiveram a sua actividade anti-haloarchaea. Contudo, *H. mediterranei* Δ*ycaO* mostrou uma inibição ligeiramente aumentada, enquanto que Δ*haloA* mostrou uma actividade ligeiramente reduzida quando comparada com a estirpe original. Assim, o BGC estudado não codifica a(s) principal(ais) molécula(s) antimicrobiana(s) produzida(s) por *H. mediterranei*, que permanecem, assim, desconhecidas. Adicionalmente, estes resultados sugerem que outro(s) peptídeo(s)/proteína(s), e não exclusivamente HaloA, pode(m) ser um substrato para a enzima YcaO. Logo, serão necessários mais estudos para caracterizar as moléculas antimicrobianas produzidas por *H. mediterranei*, bem como para elucidar a função celular de YcaO e HaloA.

keywords RiPPs, secondary metabolites, TOMMs, YcaO

abstract Halobacteria, also known as haloarchaea, is a class of halophilic Archaea living in hypersaline environments. Haloarchaea, similarly to all the extremophiles, possess a peculiar metabolism and have developed mechanisms that allow them to survive in harsh conditions, like high salinity, lack of nutrients and excessive UV exposure. Some of these adaptations lead to the production of a unique set of secondary metabolites, such as carotenoids, siderophores, polyhydroxyalkanoates, haloarchaeocins and ribosomally synthesized and post-translationally modified peptides (RiPPs). RiPPs produced by bacteria have been extensively studied because of their variety of structures and bioactivities, namely, as antibiotics, antivirals, antipain and morphogenetic compounds, but little is known about these peptides in Archaea. Recently, a group of biosynthetic gene clusters (BGCs), putatively encoding the production of RiPPs, were identified in the genome of various haloarchaea using bioinformatics tools and denominated haloazolins. These BGCs encode a cyclodehydratase belonging to the YcaO superfamily that install thiazole and oxazole heterocycles in their cognate peptides and, so far, none of them were experimentally investigated. *Haloferax mediterranei* ATCC 33500 is a haloarchaea able to inhibit growth of other haloarchaea and which encodes a haloazolisin BGC composed, at least, by the cyclodehydratase (*ycaO*) and its putative cognate peptide (*haloA*) genes. The main objective of this work was to investigate if this BGC could be involved in the anti-haloarchaea activity of *H. mediterranei*. Firstly, we have characterized *H. mediterranei* growth and the antagonistic activity along five days of growth in YPC agar, and it was concluded that maximum activity was reached after four days of incubation. At this timepoint, the transcriptional levels of *ycaO* and *haloA* were determined by RT-qPCR. Both genes were found to be transcribed, although not at the same level. Then, two knockout mutants, *H. mediterranei* Δ*ycaO* and *H. mediterranei* Δ*haloA* were generated with the pop-in/pop-out method and their antagonistic activity was tested. The deletion of the genes did not influence the production of biomass and Δ*ycaO* and Δ*haloA* mutants retained their anti-haloarchaea activity. However, Δ*ycaO* displayed a slightly increased inhibition, whereas Δ*haloA* showed a slightly reduced activity compared to the wildtype. Thus, the haloazolisin BGC does not encode the main antimicrobial molecule(s) produced by *H. mediterranei*, which remains unknown. Additionally, these results suggest that other peptide(s)/protein(s), and not exclusively HaloA, might be a substrate(s) for the YcaO enzyme. Also, they raised some doubts about whether HaloA is the cognate peptide of this enzyme. So, further experimental studies are needed to characterize the antimicrobial molecules produced by *H. mediterranei* and to understand the cellular function of YcaO and HaloA.

Table of Contents

List of Figures

List of Tables

List of Abbreviations

ADP = adenosine diphosphate
ATP = adenosine triphosphate
BGC = biosynthetic gene cluster
bp = base pair
CAM = casamino acids medium
CFU = colony forming unit
Dha = dehydroalanine
Dhb = dehydrobutyrine
DNAPol = DNA Polymerase
dNTPs = deoxyribonucleotide triphosphate
dUTP = deoxyuridine triphosphate
HalH1 = halocin H1
HalH4 = halocin H4
HalH6/H7 = halocin H6/H7
kDa = kilo Dalton
Lan = lanthionine
LAPs = linear azol(in)e-containing peptides
MCR = methyl-coenzyme M reductase
MCS = multiple cloning site
MeLan = 3-methyllanthionine
MRSA = methicillin-resistant *Staphylococcus aureus*
OD = optic density
ORF = open reading frame
PCR = Polymerase Chain Reaction
PHAs = Polyhydroxyalkanoates
PTMs = post-translational modifications
qPCR = quantitative Polymerase Chain Reaction
REE = RiPP-precursor recognition element
rpm = revolutions per minute
RiPPs = ribosomally synthesized and post-translationally modified peptides
RT-qPCR = real-time quantitative PCR
Tat = twin-arginine translocation
TOMMs = thiazole/oxazole-modified microcins

UDG = Uracil-DNA glycosylases

UV = ultraviolet

VRE = vancomycin-resistant enterococci

YPC = Yeast-Peptone-Casamino acids

YPCss = Yeast-Peptone-Casamino acids super-salted

1. Introduction

What are Archaea?

Archaea is the most recently identified of the three domains of life. The term "archaebacteria" was used for the first time in 1977 (only 45 years ago) by Carl Woese to describe methanogenic bacteria. While working on ribosomal RNA sequencing of several bacteria, Woese noticed that, even if methanogens were prokaryotic cells, their 16S rRNA was different from that of both "typical" bacteria; therefore, he proposed to introduce a third domain of life (C. R. Woese & Fox, 1977; C. R. Woese, Magrum, Fox, Magrum, & Balch, 1978).

The name "archaebacteria" is due to these organisms' characteristics and metabolism, which could have allowed them to dominate the early Archean Eon (3-4 billion years ago): in an age when living conditions were characterized by a warm and reducing atmosphere, methanogenesis might have represented a primordial form of "respiration" (C. R. Woese, Magrum, & Fox, 1978).

Further researches on 16S rRNA sequencing revealed that also extreme halophiles, belonging to the genus *Halobacterium* and *Halococcus*, and thermoacidophiles, namely *Sulfolobus* and *Thermoplasma*, were included in the domain Archaea (C. R. Woese, Magrum, & Fox, 1978). When they were discovered, archaea were thought to live only in "specialized" or "extreme" habitats; nowadays, it is known that this domain is constituted on phenotypically varied prokaryotic organisms that live in the most diverse circumstances (Chaban, Ng, & Jarrell, 2006).

1.1.1. Common features of the Archaea domain

Archaea are prokaryotes, but they differ from bacteria in many structural features that include:

i) Archaea's cell walls lack peptidoglycan and the cells are frequently covered by a proteinaceous coat, also called S-layer (Klingl, Pickl, & Flechsler, 2019);
ii) Archaeal transcription factors constituting the pre-initiation complex and the RNA polymerase structure are eukaryotic-like, while the transcriptional regulators, such as repressors and activators, are more similar to the bacterial ones (Gehring, Walker, & Santangelo, 2016; Jun, Reichlen, Tajiri, & Murakami, 2011);
iii) Archaea's genome is organized in histones, whose quaternary structure forms filaments called hypernucleosomes (Henneman, van Emmerik, van Ingen, & Dame, 2018);
iv) Archaeal phospholipids are constituted by glycerol-1-phosphate ether-linked to isoprenoid chains (Corcelli, Chong, & Koga, 2012).

1.1.2. Tree of Life: the archaeal branch

The major obstacle for Archaea's classification is that a great part of these microorganisms cannot be cultured in laboratory. In fact, according to Rule 18a of the International Code of Nomenclature on Prokaryotes (ICNP), a fundamental characteristic to describe a strain or a species is that they should be maintained in pure culture. However, In the last 20 years, cultivation-independent approaches, such as metagenomics-based and single-cell genomics methods, have allowed to sequence the genomes of non-cultivable organisms. All of this genetic information has been used for the construction of phylogenetic trees. Specifically, the Archaea domain was proposed to be divided into 4 major groups, or super-phyla (Figure 1): Asgard, DPANN group, Euryarchaeota and TACK group (Castelle & Banfield, 2018).

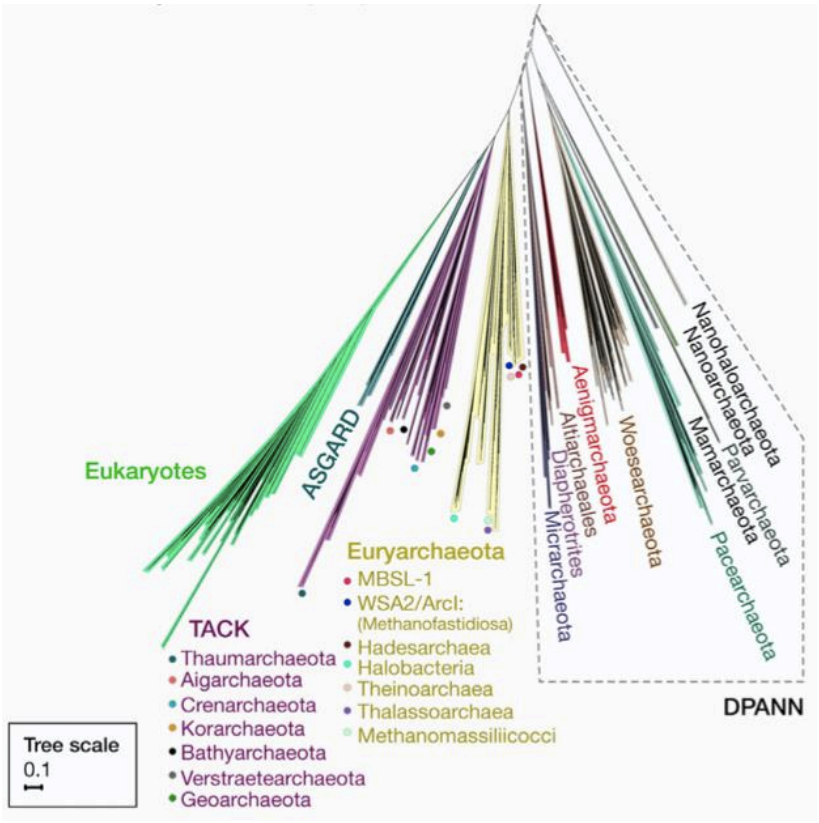

Figure 1. Tree for Archaea domain (Castelle & Banfield, 2018).

1.1.3. The landscape of archaeal habitats

From the 90's until today, 16S rRNA analyses on microbial samples, collected from a variety of both extreme and ordinary environments, have led to the conclusion that representatives of the Archaea domain are present everywhere. In fact, Archaea can be found in volcanos, hydrothermal vents, salt marshes and lakes, solfataras, deep seas; but

also in ocean waters, marine sediments, estuaries, various animals' gut and soil (Chaban et al., 2006).

Lately, archaea have been found to colonize also the human body, leading to the adoption of the word "archaeome" to define the archaeal portion of the microbiome. Organisms belonging to the human archaeome were isolated from the respiratory tract (nose and lung), the digestive tract (mouth and gut), the vaginal cavity and the skin (Koskinen et al., 2017; Pausan et al., 2019). Interestingly, together with the methanogens, representatives of the class Halobacteria, hence halophilic archaea, were identified into the human gut and it was found that changes in the archaeome constitution could be associated with some pathologies (Chibani et al., 2020; Coker, Wu, Wong, Sung, & Yu, 2020; Kim et al., 2020).

1.2. The class Halobacteria: the haloarchaea

Among the Archaea domain, halophilic archaea constitute a group of organisms with interesting characteristics and one of them, namely *Haloferax mediterranei*, described at section 1.2.1, is the focus of the present work. Halophilic archaea, also known as haloarchaea, are extreme halophiles and belong to the class Halobacteria (phylum Euryarchaeota), which includes three orders (Halobacteriales, Haloferacales, and Natrialbales) and six families (Gupta, Naushad, Fabros, & Adeolu, 2016).

Organisms living in saline environments are divided into three categories: extreme halophiles, that grow optimally at 2.5 – 5.0 M salt, moderate halophiles growing better at 0.5 – 2.5 M salt, and halotolerants, that do not need high salinity to survive but are able to tolerate salt concentrations up to 2.5 M (Oren, 2008). Halophilic microorganisms adapted their metabolism and physiology in order to contrast the harsh conditions they live in, namely nutrient starvation, elevated UV radiation, lack of water and high ionic strength (Torregrosa-Crespo, Galiana, & Martínez-Espinosa, 2017).

In general, halophiles use two different approaches in order to maintain the osmotic balance between the interior and exterior of the cell: the "low-salt-in" and the "salt-in" strategies. The first one is the most used among bacteria and eukaryotes and it consists in the accumulation of organic compounds, like amino acids and sugars, that act like osmotic solutes, allowing the exclusion for the cytoplasm. While the "salt-in" strategy, the most used among haloarchaea, consists in the accumulation of potassium chloride (KCl) inside the cell, resulting in changes in the enzymatic machinery and the presence of a highly acidic proteome (Oren, 2008).

Additionally, metagenomic analysis revealed that halophilic organisms belonging to all three domains of life possess salt-resistance genes, encoding for: i) glycerol permease and a proton pump, both known to be involved in osmoadaptation, and ii) proteins involved in nucleic acid repair, replication and transcription (Mirete et al., 2015). Specifically, several universal stress proteins (USPs) with divergent functional and catalytic motifs, such as amino acid permeases and a Na+/H+ exchanger, were found in haloarchaeal genomes (Matarredona, Camacho, Zafrilla, Bonete, & Esclapez, 2020).

Furthermore, haloarchaea undergo a strong oxidative stress, due to the desiccation environment and the elevated UV exposure that characterizes their habitats (Giani & Martínez-Espinosa, 2020). In order to cope with these conditions, they developed several strategies, such as i) DNA repair mechanisms (Jones & Baxter, 2017), ii) synthesis of carotenoids as photoprotectors (Calegari-Santos, Diogo, Fontana, & Bonfim, 2016), and iii) synthesis of polymers for carbon and energy storage (Obruca, Sedlacek, Koller, Kucera, & Pernicova, 2018).

All haloarchaea analysed to date have been found to be polyploid, therefore possessing more copies of the chromosome; a characteristic that allows these organisms to be more resistant to situations that induce DNA double-strand breaks, such as X-rays irradiation and desiccation (Zerulla & Soppa, 2014).

Because of the metabolic adaptations due to the environmental conditions they live in, haloarchaea are able to produce enzymes and primary and secondary metabolites of biotechnological interest.

1.2.1. *Haloferax mediterranei* characterization

Haloferax mediterranei R4 (ATCC 33500) is an extreme halophilic archaeon that was isolated from a salt pond in Alicante, Spain, in 1980 (Rodriguez-Valera, Ruiz-Berraquero, & Ramos-Cormenzana, 1980). It is an aerobic, pink-pigmented microorganism (Rodriguez-Valera, Juez, & Kushner, 1982) belonging to the Haloferacaceae family, within the order Haloferacales (Gupta et al., 2016).

H. mediterranei is quite resistant to environmental stressful conditions. In fact, it is able to grow in a salinity range of 10-32.5% (*w/v*), at temperatures between 32°C and 52°C, in the range 5.75-8.75 of pH, and under high metal concentrations (Matarredona et al., 2021).

This haloarchaeon is considered a model organism for studies on archaea, particularly on haloarchaea, due to several features:

i) among the known species of Halobacteriaceae, *H. mediterranei* is the one that grows faster (Oren & Hallsworth, 2014);

ii) it is metabolically versatile; it is able to grow both on simple and complex media, and to use different organic substrates as carbon source (Oren & Hallsworth, 2014);
iii) it is an aerobic organism but can live anaerobically, both through denitrification (R. M. Martínez-Espinosa, Richardson, Butt, & Bonete, 2006) and using alternative electron acceptors, such as chlorate and perchlorate (Rosa María Martínez-Espinosa, Richardson, & Bonete, 2015);
iv) its genome has been completely sequenced (Han et al., 2012);
v) gene-knockout systems for *H. mediterranei* genetic manipulation exist and are efficient (Castro, 2019; Liu, Han, Liu, Zhou, & Xiang, 2011).

From a biotechnological point of view, *H. mediterranei* has two great advantages: in the first place, it is a source of secondary metabolites that could find application in many areas - such as the production of organic-solvents-resistant enzymes for industrial use, bioremediation of wastewaters and soil and synthesis of compounds for biocompatible plastics fabrication (Matarredona et al., 2021) - and, additionally, it is a promising cell factory for the production of diverse compounds (Mitra, Xu, Xiang, & Han, 2020; Zuo et al., 2018).

Another characteristic of *H. mediterranei* is the inhibitory activity against other haloarchaea (Figure 2), that is caused by a proteinaceous compound (Rodriguez-Valera et al., 1982). For decades it was thought that halocin H4, discussed in sections 1.2.2.4 and 2.1, was responsible for the inhibition observed, but it turned out that knockout mutants for halocin H4 gene (*halH4*) retained their activity (Naor, Yair, & Gophna, 2013).

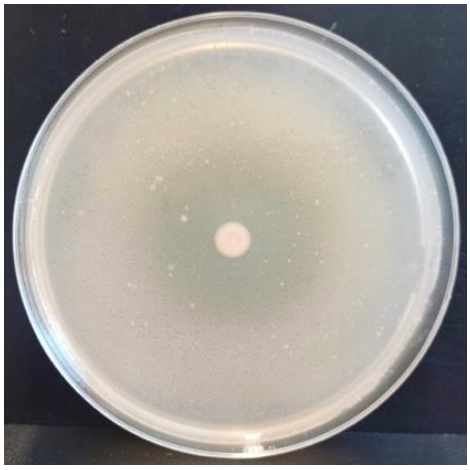

Figure 2. *H. mediterranei* WR510 inhibition halo against *H. volcanii*.

1.2.2. The secondary metabolites of haloarchaea

Haloarchaea secondary compounds, such as carotenoids, siderophores, polyhydroxyalkanoates (PHAs), haloarcheocins and ribosomally synthesized and post-translationally modified peptides (RiPPs) are worth to be investigated because of their potential applications in several fields, that will be discussed in specific sections.

Specifically, our interested is focused on the latter, RiPPs, which have been extensively studied in bacteria, but very little in archaea.

1.2.2.1. Carotenoids

Carotenoids are natural isoprenoid pigments produced by representatives of all domains of life and they can be commonly found in haloarchaea, where they are responsible for their pinkish to reddish pigmentation (Charlesworth & Burns, 2015). The most abundant carotenoids produced by haloarchaea are bacterioruberin and its derivates (Heider, Peters-Wendisch, Wendisch, Beekwilder, & Brautaset, 2014), whose main role is to protect these halophilic microorganisms from oxidative stress damages caused by the excessive UV radiation exposure (Giani & Martínez-Espinosa, 2020).

Carotenoids are compounds of great interest for the food industry, in which they find application as colouring agents and food supplements (Chandi & Gill, 2011). Moreover, they are thought to be important for human health both for they antioxidant activity and for the prevention of chronic diseases and cancer (Eggersdorfer & Wyss, 2018).

Recently, engineered *H. mediterranei* has shown to be able to produce high quantities of lycopene (Zuo et al., 2018) and another work has shed light on carotenogenesis pathway in haloarchaea, even though its regulation still has to be investigated (Giani, Miralles-Robledillo, Peiró, Pire, & Martínez-Espinosa, 2020).

The carotenoid metabolism and its regulation in halophilic archaea are still poorly explored, but the over-pigmented haloarchaea, especially *H. mediterranei*, seem promising candidates to be used as cell factories for carotenoid production (Rodrigo-Baños et al., 2021).

1.2.2.2. Siderophores

Siderophores are ion chelators, small organic molecules that are able to improve iron bioavailability. They are produced by aerobic microorganisms and released in the environment where they chelate iron, specifically Fe^{3+}, by forming complexes with it, which is internalized within the cytoplasm of the microorganisms (Hider & Kong, 2010).

These secondary metabolites are of particular interest for the agriculture and bioremediation areas because, respectively: i) some siderophores are able to enhance plant growth and health, providing them with iron and protecting them from the pathogens, actuating like environment-friendly pesticides (Glick, 2012), and ii) various bacterial siderophores showed the ability of complexing metals other than iron (Schalk, Hannauer, & Braud, 2011), leading to the hypothesis that they could be used for soil bioremediation (Ahmed & Holmström, 2014).

Siderophores have been studied among several groups of bacteria, plants and fungi (Årstøl & Hohmann-Marriott, 2019; Barry & Challis, 2009), but only a little is known about archaeal siderophores. *Nitrosopumilus maritimus* SCM1, a marine ammonia-oxidizing archaeon, was found to be able to uptake iron thanks to exogenous siderophores (Shafiee, Snow, Zhang, & Rickaby, 2019), while five species of haloarchaea were described as capable of producing endogenous ones (Dave, Anshuman, & Hajela, 2006).

Recently, it was published the first experimental study on siderophore biosynthesis genes in an archaeal species, which revealed that *Haloferax volcanii* genome contains six genes that are involved in siderophore biosynthesis, and four of them, the *iuc* (iron uptake chelate) genes, are necessary for siderophores' production (Niessen & Soppa, 2020). The authors proposed a possible siderophore biosynthetic pathway and investigated the presence of the Iuc proteins among archaea and bacteria, from which emerged that the four Iuc proteins were detected only among the haloarchaea group (Niessen & Soppa, 2020).

1.2.2.3. Polyhydroxyalkanoates (PHAs)

PHAs can be produced by microorganisms and function as a source of carbon and energy in the form of insoluble inclusions in the cytoplasm. From the chemical point of view, they are linear polyesters, constituted by hydroxy acid monomers linked by an ester bond (Philip, Keshavarz, & Roy, 2007).

In the last years, interest in PHAs has increased because of their similarities with the petrochemical polymers. In fact, they might have industrial applications as a source of biodegradable and biocompatible polymers.

While PHAs have been widely studied among the bacteria, there is a very limited knowledge regarding these compounds in the domain Archaea. Nevertheless, representatives of several haloarchaeal genus have showed to produce PHAs (Poli, Di Donato, Abbamondi, & Nicolaus, 2011). The most studied genus are *Haloarcula* and *Haloferax*, which have emerged as good candidates for PAHs production since they have some advantages over bacteria, including their simple growth requirements and the need

of high salinity that prevents culture contaminations. Moreover, the biopolymers could be easily separated with low salinity media or distilled water, instead of using solvents for their extraction (Torregrosa-Crespo et al., 2017).

1.2.2.4. Haloarcheocins

Bacteriocins are antimicrobial proteins and peptides produced by both Gram-positive and Gram-negative bacteria that are able to kill close relatives of the producing strain. Analogously, antimicrobial peptides/proteins produced by members of the Eukarya domain are called “eucaryocins” and archaeal bacteriocins are known as “archaeocins” (O’Connor & Shand, 2002). Archaeocins include two groups of antimicrobial proteins/peptides (AMPs), namely halocins (or haloarcheocins) and sulfolobicins, and their first report backs to 1982 (Rodriguez-Valera et al., 1982), when halocins were firstly described. At the time, halocins production showed to be a common feature among haloarchaea (Marina Torreblanca, Meseguer, & Ventosa, 1994). Their ecological role would be to reduce competition among strains that live in the same habitat. They might act by inducing the lysis of the competitor, which would provide more nutrients for their producer (O’Connor & Shand, 2002).

Originally, six types of halocins were proposed, from H1 to H6 (Rodriguez-Valera et al., 1982). Nowadays, they are known to be a large and heterogeneous group of compounds that widely differs in spectrum of activity, salt dependence and tolerance to temperature (Table 1). Halocins also vary in their size, going from 3.6 kDa to 35 kDa; therefore, when smaller than 10 kDa, they are called “microhalocins” (Table 2). Microhalocins are, in general, hydrophobic and robust, resistant to many organic solvents and to temperature and salt concentration variations (O’Connor & Shand, 2002).

Some halocins, namely H4, S8 and C8, are synthesized as a longer pre-peptide, that suffer at least one proteolytic cleavage, even though the details are not known yet (Besse, Peduzzi, Rebuffat, & Carré-Mlouka, 2015). Regarding their mechanism of action, HalH4 and HalH1 seem to modify the membrane permeability, but it is still unclear how (I. Meseguer & Rodriguez-Valera, 1986; Gonzalo Platas, Meseguer, & Amils, 2002) and HalH6/H7 is known to inhibit the Na^+/H^+ antiporter (Inmaculada Meseguer, Torreblanca, & Konishi, 1995). In the end, some halocins, namely H4 and S8, showed a N-terminus Tat sequence, suggesting that their transport could be mediated by the Tat-pathway (Palmer & Berks, 2012).

Table 1. List of halocins that have been characterized so far (adapted from (Kumar & Tiwari, 2019).

Halocin	Producer	Size	Thermal stability	Salt dependence	Activity spectrum	References
H1	*Haloferax mediterranei* M2a (previously Xia3)	31 kDa	< 50°C	> 10%	Broad	(G. Platas, Meseguer, & Amils, 1996; Gonzalo Platas et al., 2002; Rodriguez-Valera et al., 1982)
H2	Haloarchaeon Gla2.2	ND	ND	ND	Broad	(Rodriguez-Valera et al., 1982)
H3	Haloarchaeon Gaa12	ND	ND	ND	Broad	(Rodriguez-Valera et al., 1982)
H4	*Haloferax mediterranei* R-4 (ATCC 33500)	39.6 kDa (pre-protein), 34.9 kDa (mature)	< 60°C	> 15%	Broad (particularly active against *Halobacterium salinarum*)	(Cheung, Danna, O'Connor, Price, & Shand, 1997; Rodriguez-Valera et al., 1982)
H5	Haloarchaeon Ma2.20	ND	ND	ND	Narrow	(Rodriguez-Valera et al., 1982)
KPS1	*Haloferax volcanii* KPS1	ND	< 80°C		Broad (including haloarchaea, Gram-positive and Gram-negative bacteria)	(Kavitha P. , Lipton A.P., 2011)
Sech7a	*Haloferax mediterranei* Sech7a	10.7 kDa	< 80°C	> 5%	Narrow	(Pašić, Velikonja, & Ulrih, 2008)
SH10	*Natrinema* sp. BTSH10	20 kDa	< 50°C	ND	ND, it is very active against *Halorubrum* sp. BTSH3	(Karthikeyan, Bhat, & Chandrasekaran, 2013)
HA1	*Haloferax larsenii* HA1	14 kDa	<100°C	> 10%	Narrow (inhibits only *Haloferax larsenii* HA3, HA4, HA9 and HA10)	(Kumar, Saxena, & Tiwari, 2016)
HA3	*Haloferax larsenii* HA3	13 kDa	< 80°C	> 10%	Narrow (inhibits only *Haloferax larsenii* HA10)	(Kumar & Tiwari, 2017)
HA4	*Haloferax larsenii* HA4	14 kDa	<100°C	> 10%	Narrow (inhibits only *Haloferax larsenii* HA1, HA3, HA8, HA9 and HA10)	(Kaur & Tiwari, 2021)

Table 2. List of microhalocins that have been characterized so far (adapted from (Kumar & Tiwari, 2019).

Halocin	Producer	Size	Thermal stability	Salt dependence	Activity spectrum	References
A4	Strain TuA4	7.4 kDa	< 90°C	Not salt-dependent	Broad (also active against *Sulfolobus* spp.)	(Haseltine et al., 2001)
C8	*Natrinema* spp. AS7092 (previously *Halobacterium* AS79092)	6.3 kDa	> 100°C	Not salt-dependent	Broad	(Y. Li, Xiang, Liu, Zhou, & Tan, 2003)
H6/H7	*Haloferax gibbonsii* Ma2.39 (or Alicante SPH7)	~ 3 kDa (or 32 kDa, not clear yet)	< 90°C	Not salt-dependent	Narrow (particularly active against *Halobacterium salinarum*)	(Rodriguez-Valera et al., 1982; M. Torreblanca, Meseguer, & Rodriguez-Valera, 1989)
R1	*Halobacterium salinarum* GN101	3.8 kDa	<60°C	Not salt-dependent	Broad (also active against *Sulfolobus* spp., and *M. thermophila*)	(Ebert, Goebel, Moritz, Rdest, & Surek, 1986; Haseltine et al., 2001; O'Connor & Shand, 2002)
S8	Haloarchaeon S8a (Great Salt Lake, UT)	3.58 kDa	< 93°C	Not salt-dependent	Broad (inhibiting *Hfx. gibbonsii*, *Halobacterium* spp., and *Sulfolobus* spp.)	(Haseltine et al., 2001; Price & Shand, 2000)

1.2.2.5. Ribosomally synthesized and post-translationally modified peptides (RiPPs)

RiPPs are a large group of natural products of a maximum molecular weight of 10 kDa and whose biosynthetic gene clusters (BGCs) have been identified in all three domains of life. They are initially synthesized as a precursor peptide (Figure 3A), of about 20-100 residues in length, which undergo several post-translational modifications (PTMs) by a characteristic set of enzymes (Figure 3B), depending on the class (Arnison et al., 2013).

Specifically, the part of the precursor peptide that is modified and originates the mature peptide is called core peptide (Figure 3A). The precursor peptide can include some other optional sequences: i) the leader peptide, which could be important for the recognition by the biosynthetic enzymes, ii) the signal sequence that is present in some eukaryotic peptides and directs the peptide to a specific cellular compartment, and iii) the recognition sequence, which is important for the excision and cyclization of some classes of RiPPs

(Oman & Van Der Donk, 2010). At the end of the biosynthetic process, the precursor peptide suffers a proteolytic removal of all these accessory sequences in order to produce a fully modified and functional mature peptide (Figure 3B) (Arnison et al., 2013; Russell & Truman, 2020).

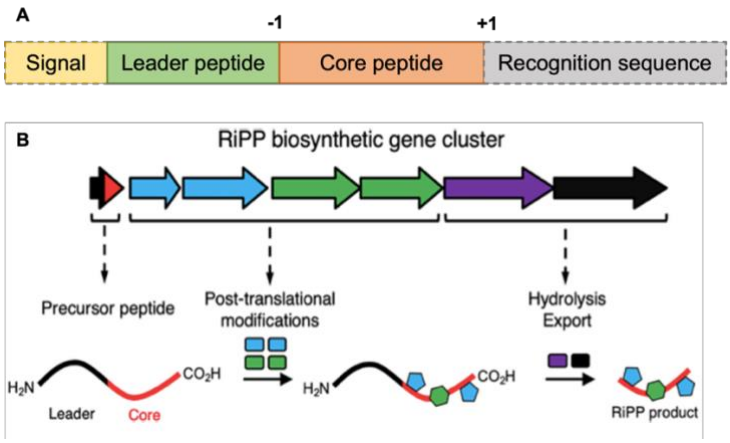

Figure 3. A) Representation of the general structure of precursor peptides in RiPPs. B) General RiPP biosynthetic gene cluster and schematic representation of RiPP biosynthesis (Russell and Truman, 2020).

RiPPs are a family of peptides with a vast diversity and structural and chemical complexity. Consequently, they can assume several functions and can be an enormous source of new compounds to investigate. RiPPs have been widely studied in bacteria and only recently, thanks to genome mining technologies, they were identified in archaeal genomes.

1.3. RiPPs in haloarchaea

Biosynthetic gene clusters (BGCs) belonging to different classes of RiPPs were found in archaeal genomes by genome mining, including lanthipeptides (Costa, 2017; Walker et al., 2020), lasso peptides (Maksimov, Pelczer, & Link, 2012), and haloazolisins (Cox, Doroghazi, & Mitchell, 2015). From these, only lanthipeptides and haloazolisins were identified in haloarchaeal genomes. The present work will focus on this last class, whose gene cluster has been found in several haloarchaeal genomes, but has never been experimentally studied.

1.3.1. Lanthipeptides

The compound of the lanthipeptide's class to be described is nisin, produced by *Lactococcus lactis*, which first report back to 1928 (Rogers, 1928), but it was characterized

only in 1971 (Gross & Morell, 1971). The PTMs that define lanthipeptides are the meso-lanthionine (Lan) and 3-methyllanthionine (MeLan) that are formed in two steps (Figure 4):

i) Dehydration of some or all serine (Ser) and threonine (Thr) of the core peptide to dehydroalanine (Dha) and dehydrobutyrine (Dhb), respectively;

ii) Conjugate addition of cysteine (Cys) thiols to Dha and Dhb residues, resulting in Lan and MeLan formation, respectively (Repka, Chekan, Nair, & Van Der Donk, 2017).

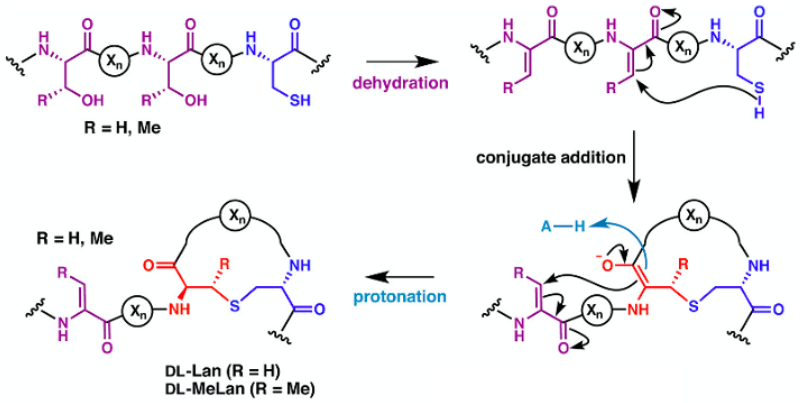

Figure 4. General scheme for Lan and MeLan formation (Repka et al., 2017).

Currently four classes of lanthipeptides are known, and they differ in the biosynthetic enzymes that lead to the (Me)Lan formation (Figure 5). For class I lanthipeptides, dehydration and cyclization are carried out by two separate enzymes, namely LanB and LanC; while, for classes II, III, and IV they are carried out by bifunctional lanthionine synthetases (Arnison et al., 2013).

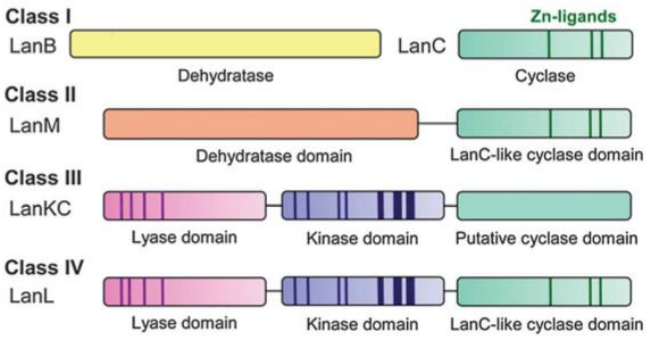

Figure 5. Representation of the domains that characterize the different classes of lanthipeptide's synthetases. (Arnison et al., 2013).

Gene clusters of class II lanthipeptides, compounds known for their antimicrobial activity (Arnison et al., 2013), were identified by genome mining in haloarchaeal genomes. However, the biosynthetic pathway of none of them was experimentally investigated and it

remains unclear if their bioactivity is similar to those produced by bacteria or if they have other functions (Castro, 2019; Walker et al., 2020). The only existing experimental study regarding haloarchaea and lanthipeptides was performed with *Haloferax mediterranei* ATCC 33500. Different knockout mutants without the lanthipeptide's synthetase genes were tested against other haloarchaea, but they retained their inhibitory activity indicating that *H. mediterranei* antiarchaeal activity is not due to lanthipeptides (Castro, 2019).

1.3.2. Thiazole/oxazole-modified microcins (TOMMs)

This thesis will focus on haloazolisins, a term coined by Cox et al. (2015) to define a group of thiazole/oxazole-modified microcins (TOMMs) BGCs found in haloarchaea by genome mining (Cox et al., 2015). TOMMs are group of RiPPs characterized by heterocycles derived from cysteine (Cys), serine (Ser) and threonine (Thr) residues (Melby, Nard, & Mitchell, 2011).

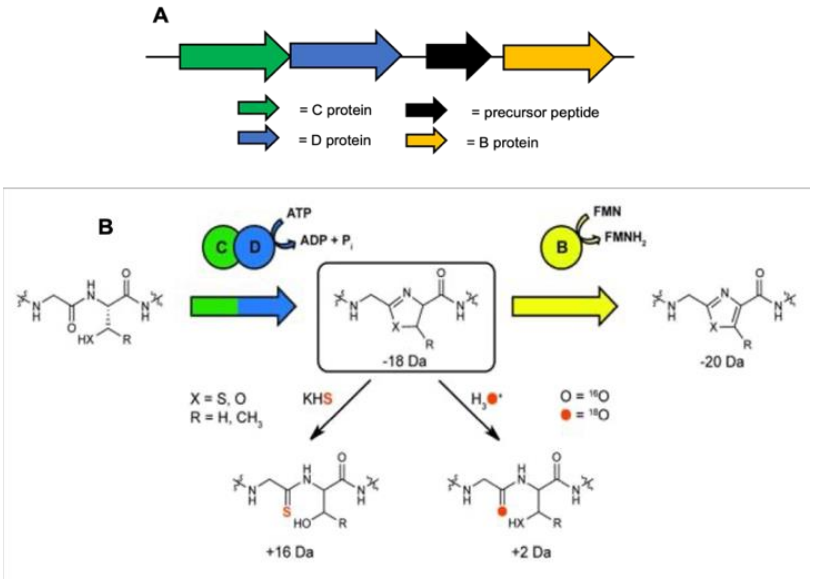

Figure 6. A) Representation of a generic BGC of a TOMM. C and D protein (YcaO protein) are usually found truncated. B) General scheme for Ser, Cys or Thr heterocyclization to form azol(in)es (Dunbar & Mitchell, 2013).

The PTMs of TOMMs are catalysed by a cyclodehydratase, composed by a member of the YcaO superfamily (D protein) and by a E1 ubiquitin-activating enzyme homolog (C protein) (Figure 6A). The YcaO protein catalyses the cyclodehydration reaction of Cys, Ser and Thr, while the C protein seems to be involved in recognizing the leader peptide and by potentiating the reaction. These two proteins can be found encoded by two different genes or be fused in a single ORF. A (FMN)-dependent dehydrogenase (B protein) can be also involved in TOMM's biosynthesis, since they oxidize azoline rings to azoles (Figure 6B)

(Cox et al., 2015; Dunbar & Mitchell, 2013). Depending on the TOMM's structure, other modification enzymes can be involved in their biosynthesis. Representatives of TOMMs have been extensively studied and characterized in bacteria, such as microcin B17 produced by *E. coli* (Yorgey et al., 1994) and streptolysin S produced by *Streptococcus pyogenes* (Mitchell et al., 2009)

Haloazolizin's BGCs were detected by *in silico* analysis since they encode a fused cyclodehydratase composed by a full YcaO domain and a barely recognizable C protein domain in its N-terminus (Cox et al., 2015). The BGCs were proposed to be involved in the biosynthesis of TOMMs but it is still unknown if YcaO enzyme is indeed involved in the production of TOMMs (or other type of RiPPs), or if they play other cellular roles.

YcaO superfamily, previously identified as DUF181 (domain of unknown function) proteins, includes several proteins distributed across bacteria and archaea. In 2014, they were classified into three groups: i) TOMM, ii) non-TOMM and iii) TfuA non-TOMM (Dunbar et al., 2014). ATP utilization is a universal feature of these three groups, which are therefore characterized by a conserved ATP-binding motif, as shown in Figure 7 (Dunbar et al., 2014).

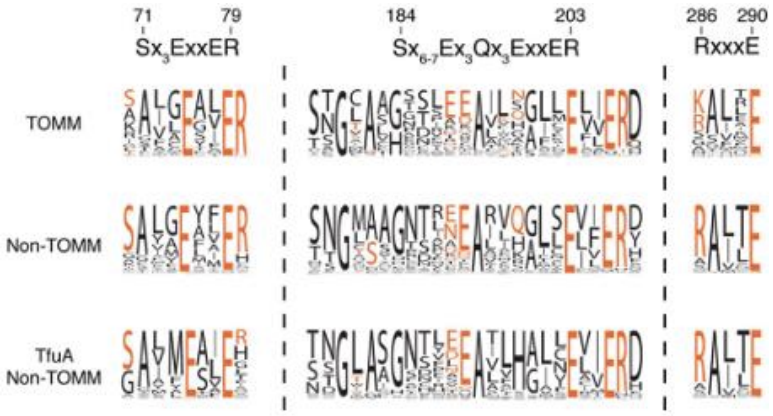

Figure 7. Sequence logo plot showing the conservation of the ATP-binding motif in the different members of YcaO superfamily (Dunbar et al., 2014).

YcaOs catalyse the formation of three types of modifications: i) azoline, ii) macroamidine and ii) thioamide (Figure 8). In the last years, it was proposed that these three types of reactions might proceed with the same mechanism of action (Burkhart, Schwalen, Mann, Naismith, & Mitchell, 2017). The hypothesis is that it starts with a nucleophilic attack at the amide carbonyl carbon, and it would be the nature of the nucleophile (Ser/Thr/Cys lateral chain, $-NH_2$ from amide, or a S-containing-cofactor) to determine the final product (Figure 8). This causes the formation of a tetrahedral oxyanion intermediate, that allows the attack of ATP and the consequent release of ADP. In the end, the intermediate collapses causing

the formation of the final product and the release of phosphate as a by-product (Burkhart et al., 2017; Franz, Kazmaier, Truman, & Koehnke, 2021; Montalbán-López et al., 2020).

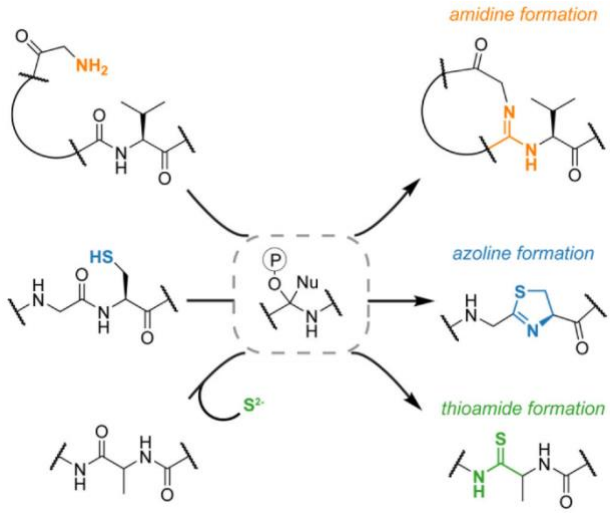

Figure 8. Simplified representation of the mechanism proposed for azoline, thioamide and macrolactamidine formation catalysed by YcaOs (Burkhart et al., 2017).

YcaOs are responsible for the installation of PTMs in five classes of RiPPs: thiopeptides, linear azol(in)e-containing peptides (LAPs), thioamitides, cyanobactins and bottromycins (Montalbán-López et al., 2020). From these, TOMMs include thiopeptides, LAPs, cyanobactins and bottromycins (Cox et al., 2015).

It is still unknown if the YcaO proteins encoded in haloazolisins' BGCs are truly involved in the biosynthesis of RiPPs, and, if so, which type of RiPPs they are modifying. Therefore, it is important to understand the differences among the classes of RiPPs that involve the action of YcaOs, which will be discussed in the following sections.

1.3.2.1. Thiopeptides

Thiopeptides are macrocyclic peptides carrying multiple thiazole rings and often containing dehydrated amino acid residues (Figure 9) with several structures and functions that include antibiotics (Chan & Burrows, 2021). Their defining chemical feature is the presence of a central pyridine, derived by the [4+2] cycloaddition of two Dha and the class-defining enzyme is the [4+2] cycloaddition enzyme (A. Hudson, Zhang, I. Tietz, A. Mitchell, & A. van der Donk, 2015). Two compounds belonging to this class of RiPPs are thiomuracin (Figure 9), produced by *Thermobispora bispora* (A. Hudson et al., 2015), and sulfomycin, produced by *Streptomyces viridochromogenes* (Du et al., 2020).

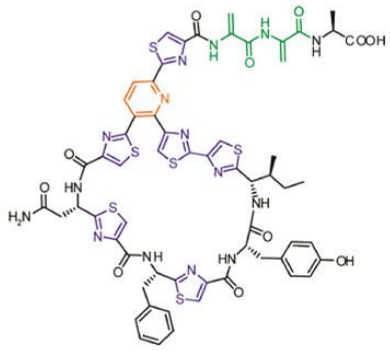

Figure 9. Representation of the thiomuracin structure produced by *Thermobispora bispora* (A. Hudson et al., 2015). Thiazole rings are in purple, the class-defining pyrimidine in red, and dehydrated amino acids residue in green.

The biosynthesis of thiopeptides (Figure 10A) occurs in different steps (A. Hudson et al., 2015; Montalbán-López et al., 2020):

i) Three enzymes, namely a RiPP-precursor recognition element (REE), cyclodehydratase (azoline-forming YcaO) and dehydrogenase, cooperate to convert Cys in thiazoles;

ii) The dehydratase operates a Ser-glutamylation, followed by the elimination of glutamate, leading to the formation of Dha;

iii) The specific [4+2] cycloaddition enzyme forms the final macrocyclic peptide.

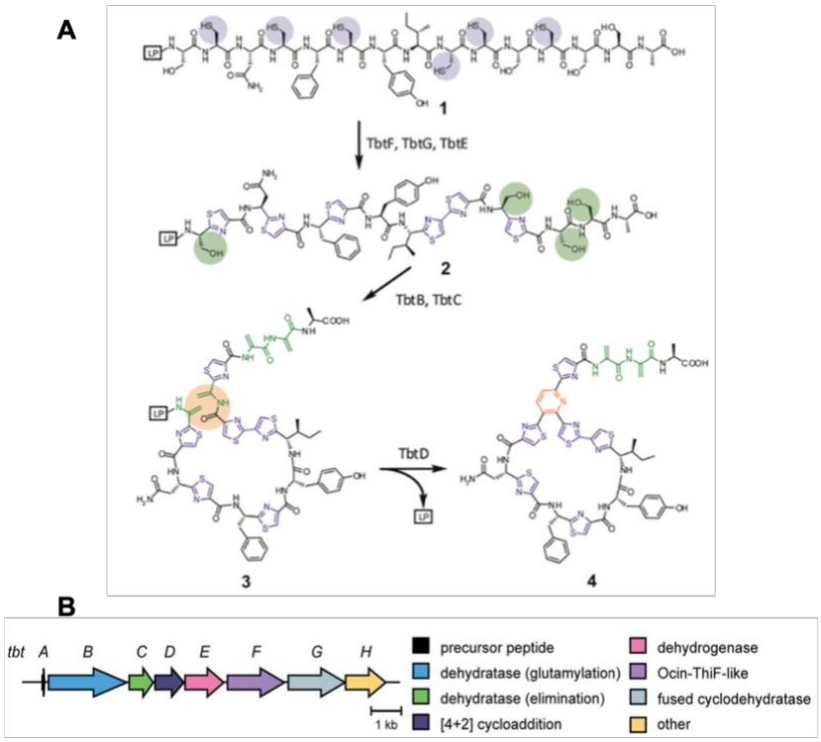

Figure 10. A) Representation of the general biosynthesis of the thiopeptide thiomuracin (A. Hudson et al., 2015). B) Biosynthetic gene cluster of thiomuracin (Montalbán-López et al., 2020).

Therefore, the minimal constitution of a thiopeptide BGC must encode: the precursor peptide, the REE, a cyclodehydratase (YcaO), a dehydrogenase, a dehydratase and a [4+2] cycloaddition enzyme (Figure 10B).

1.3.2.2. Linear azol(in)e-containing peptides (LAPs)

The defining chemical feature of LAPs is the presence of thiazol(in)e and/or (methyl)oxazol(in)e heterocycles (Figure 11), and the class-defining enzyme is the azoline-forming YcaO (Arnison et al., 2013).

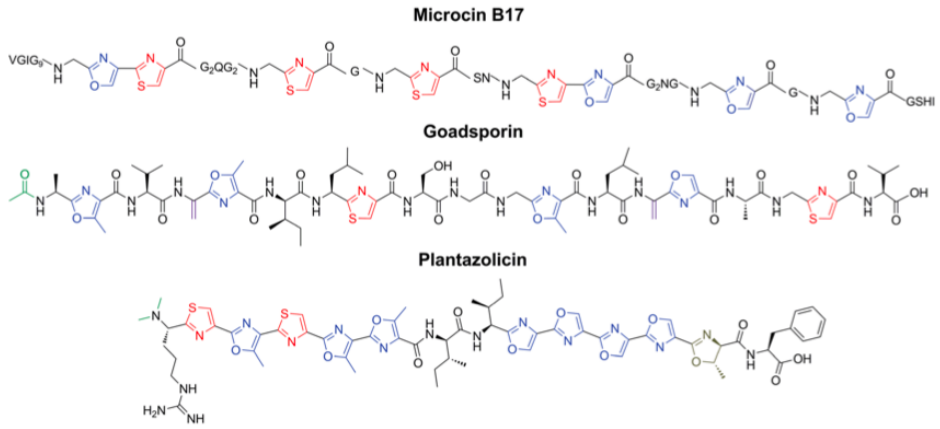

Figure 11. Chemical structures of some LAP representatives (Arnison et al., 2013).

Some members of this class of RiPPs are microcin B17 (Y. M. Li, Milne, Madison, Kolter, & Walsh, 1996), goadsporin (Igarashi et al., 2001), plantazolicin (Scholz et al., 2011) and the group of Streptolysin S-like cytolysis (Molloy et al., 2015). All LAPs characterized up to now have showed to have antibiotic activity against different targets (Arnison et al., 2013).

The main biosynthetic step of LAP production is the heterocyclization of Ser, Cys and Thr residues. This reaction is ATP-dependent and is catalyzed by the azoline-forming YcaO (Burkhart et al., 2017). Therefore, the LAP's BGCs must encode, at least, a precursor peptide and a cyclodehydratase composed by an YcaO and a E1-like protein superfamily, which can be either fused or separated into two proteins. Other genes found include dehydrogenases (oxidize azolines to azoles), proteases (eliminate the leader peptide) and transporters (Arnison et al., 2013). Examples of LAP BGCs from bacterial species are reported in Figure 12.

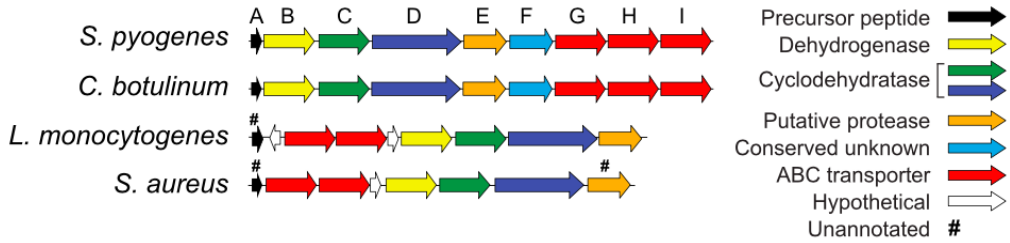

Figure 12. Example of LAP's BGCs encoding the biosynthesis of SLS-like cytolysins in different bacterial species (Molloy et al., 2015).

1.3.2.3. Thioamitides

The class-defining element for thioamitides is the presence of thioamides instead of amides in the peptide backbone (Figure 13A), and the class-defining enzyme is the thioamide-installing YcaO (Montalbán-López et al., 2020). The founding member of this class of RiPPs is thioviridamide, a compound with antiproliferative activity against cancer cells (Izawa, Kawasaki, & Hayakawa, 2013).

The thioamitide's BGCs (Figure 13B) are not well characterized, but a recent study demonstrated that an YcaO and a TfuA-like protein are necessary for the thioamides installation (Eyles, Vior, Lacret, & Truman, 2021; Montalbán-López et al., 2020). TfuA is a protein necessary for trifolitoxin synthesis, that is an antibiotic peptide produced by *Rhizobium leguminosarum bv. trifolii* strain T24. TfuA role is undefined, in fact, its name derives from the terms trifolitoxin and unknown (Breil, Borneman, & Triplett, 1996).

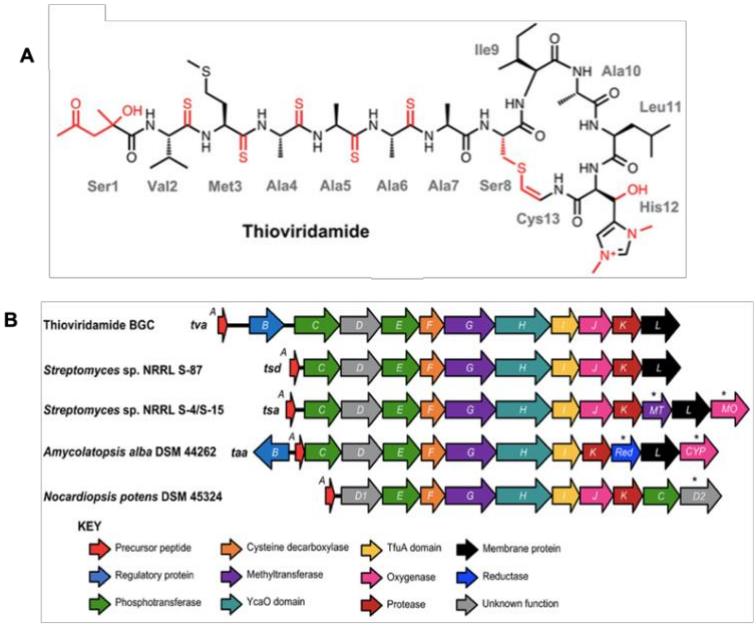

Figure 13. A) Thioviridamide chemical structure (Frattaruolo, Lacret, Cappello, & Truman, 2017). B) Thioviridamide and thioviridamide-like compounds' gene clusters (Frattaruolo et al., 2017).

1.3.2.4. Cyanobactins

Cyanobactins are a group of cytolytic peptides produced by cyanobacteria, some of the members of this group are N-to-C macrocyclized (Figure 14A) while others are linear. The first cyanobactins chemical structures were characterized in 1980 (Ireland & Scheuer, 1980), but they were recognized as a class of RiPPs only after the sequencing of the patellamide group BGCs (Figure 14B) (Schmidt et al., 2005).

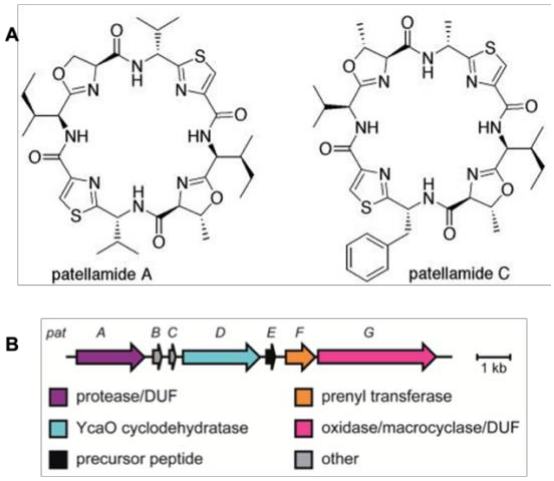

Figure 14. A) Chemical structures of patellamide A and C (Schmidt et al., 2005). B) Patellamide BGC (Montalbán-López et al., 2020).

Cyanobactins undergo several PTMs and have several chemical features, however their defining-class enzyme is the N-terminal protease. YcaO-like proteins have been found in some cyanobactins' gene clusters, but their role is to install azoline heterocycles as secondary modifications (Montalbán-López et al., 2020).

1.3.2.5. Bottromycins

Members of this class are short peptides known for their strong inhibitory activity against some antibiotic resistant bacteria, such as MRSA and VRE (Shimamura et al., 2009). Bottromycins were identified and isolated from *Streptomyces bottropensis* in 1957 (Waisvisz, Van Der Hoeven, Van Peppen, & Zwennis, 1957), but their structure was revealed only in 2009, when Bottromycins A_2 (Figure 15A) was characterized (Shimamura et al., 2009).

Even though bottromycins suffer several modifications, their class-defining chemical feature is the presence of macrolactamide (Figure 15A), and the class-defining enzyme is macrolactamide-forming YcaO. Bottromycins' gene cluster (Figure 15B) also encodes an

azoline-forming YcaO, responsible for the installing of secondary modifications (Arnison et al., 2013).

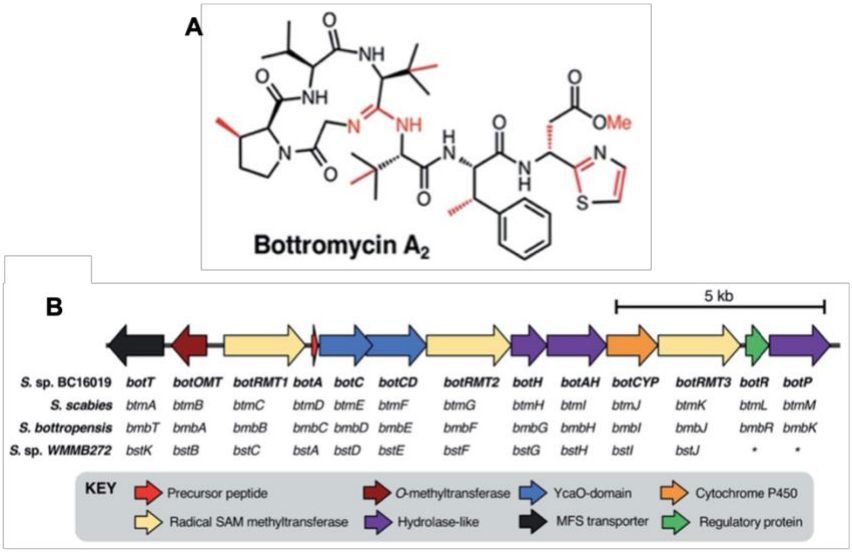

Figure 15. A) Chemical structure of Bottromycin A_2 (Franz et al., 2021). Post-translational modifications are showed in red. B) Bottromycins BGC (Franz et al., 2021).

1.3.3. Haloazolisins: do they encode the biosynthesis of TOMMs?

As abovementioned, the term haloazolisin was created to define a group of BGCs identified in the haloarchaeal genomes due to the presence of a cyclodehydratase gene (Cox et al., 2015). About 100 of these BGCs were found, and they are characterized by a fused cyclodehydratase, whose C protein domain is barely recognizable (Cox et al., 2015). At the time, it was hypothesized that the BGCs encoded the biosynthesis of TOMMs, but so far this was not experimentally confirmed.

Only 31 putative TOMM precursor peptides were predicted within the same genomes, some of which (ex: haloazolisin BGC of *Haloterrigena turkemenica*) were not found in the genetic environment of YcaO proteins, but elsewhere on the chromosome, near a protein responsible for precursor peptide binding (F-like protein; Figure 16A) (Cox et al., 2015) . The predicted precursor peptides do not share a high degree of homology, but most of them have core peptides rich in Ser residues (Figure 16B).

No more information is available until today on these compounds and are, therefore, a great opportunity to investigate the biosynthesis of natural products in archaea.

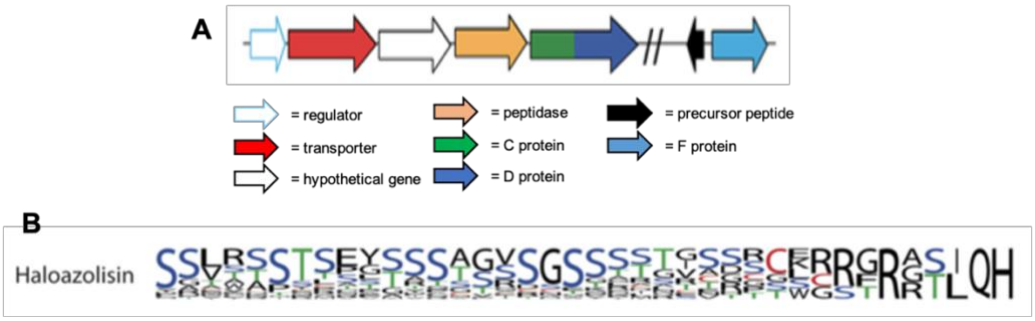

Figure 16. A) Example of a haloazolisin BGC, identified in the genome of *Haloterrigena turkmenica* DMS 5511 (Cox et al., 2015). B) Sequence logo plot of identified haloazolisins' precursor peptides (Cox et al., 2015). The D protein corresponds to the YcaO protein.

A haloazolisin BGC was identified in *H. mediterranei* ATCC 33500 and, since it is a good model organism to investigate haloarchaea (as discussed in section 1.2.1), the present work will focus on it.

The haloazolisin's report by Cox *et al.* (2015) did not analysed the BGC of *H. mediterranei* but it was considered to encode the biosynthesis of RiPPs. *H. mediterranei* genome (Figure 17) consists of one chromosome and three megaplasmids (Han et al., 2012), and this putative BCG is located on the chromosome.

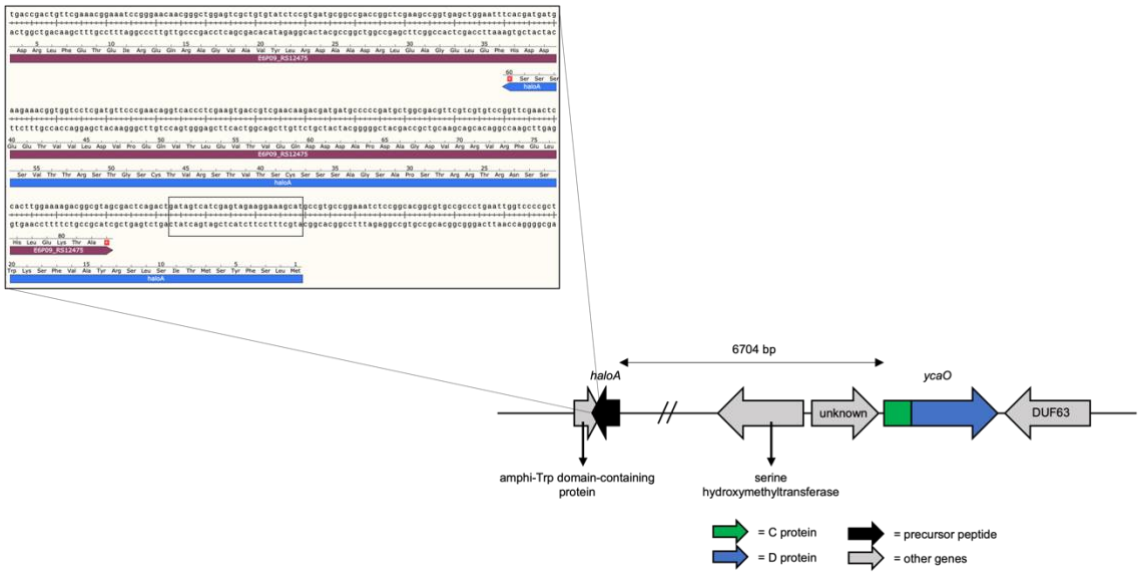

Figure 17. Representation of *H. mediterranei* haloazolisin BGC in its genetic environment. The image also highlights *haloA* sequence and, inside of that (rectangular shape), the region that was deleted to generate *H. mediterranei ΔhaloA* mutant (section 3.3.1).

Here, we adopted the universal nomenclature for RiPPs, as established by Arnison *et al.* (2013), for the percursor peptide (*haloA*; Figure 17) and the cyclodehydratase gene will be referred as *ycaO* (Figure 17). As showed in Figure 17, *ycaO* can possibly be expressed in

the same transcriptional unit of another gene of unknown function. Upstream and downstream this unit there two genes encoding a serine hydroxymethyltransferase and a protein belonging to DUF63, respectively, encoded by the opposite strand. The *haloA* predicted by Cox *et al.* (2015) is not found in the vicinity of *ycaO*, but in region approximately 6700 bp upstream (Figure 17). *HaloA* is encoded in the complementary strand and overlaps with another gene, encoding a protein containing an amphi-Trp domain, situated on the opposite strand (Figure 17).

1.4. Context and objectives of the thesis

As abovementioned, *H. mediterranei* ATCC 33500 is an haloarchaeon with several features that makes it a good model organism. Due to the harsh environment in which it lives, characterized by high salinity, lack of nutrients and high UV exposure, *H. mediterranei* has a developed several adaptations and is able to produce secondary metabolites of great interest for the industrial, food, agriculture and pharmaceutical areas.

In last years, RiPPs are emerging as an interesting source of novel natural products, with diverse chemical structures and functions. A new hypothetical group of RiPPs named haloazolisins, was identified by genome mining in haloarchaeal genomes, but it was never experimentally investigated.

Since a haloazolisin BGC was identified in *H. mediterranei* genome, it is a great opportunity to study the biosynthesis of RiPPs in haloarchaea. Specifically, many RiPPs, including TOMMs, are known for being potent antibiotics. Therefore, the main objective of this work is to investigate if the haloazolisin BGC of *H. mediterranei* encodes the biosynthesis of its antihaloarchaea compounds. In order to achieve this aim, we defined the following specific objectives:

i) Monitor *H. mediterranei* growth in agar and the trend of its antimicrobial activity along 5 days (chapter 2);

ii) Perform the transcriptional analysis of *haloA* and *ycaO* of *H. mediterranei* growth in agar (chapter 2) in order to:

- determine if they are always expressed,
- estimate their level of the expression;

iii) Generate *H. mediterranei haloA* and *H. mediterranei ycaO* knockout mutants (chapter 3);

iv) Quantify the number of viable cells and determine the transcriptional analysis of *haloA* and *ycaO* genes of the knockout mutants (chapter 4);

v) Test the antihaloarchaea activity of the mutants (chapter 4).

2. Characterization of *Haloferax mediterranei* growth, antimicrobial activity and gene transcription on agar

2.1. Introduction

Haloferax mediterranei ATCC 33500 shows an inhibitory activity against other haloarchaea (Figure 2), which was reported for the first time in 1982 (Rodriguez-Valera et al., 1982). This activity was attributed to halocin H4, which belongs to a group of antimicrobial proteins and peptides that are a practically universal feature among haloarchaea (Marina Torreblanca et al., 1994).

Halocin H4 structure and gene cluster are well-characterized and its activity was studied using *Halobacterium salinarum*, previously known as *H. halobium*, and *Haloferax volcanii* as an indicator strains (I. Meseguer & Rodriguez-Valera, 1986; Naor et al., 2013). HalH4 is sensitive to salt-concentration, temperature and proteases. Specifically, it is able to maintain its activity at salinity higher than 15 % and up to 60°C (Rodriguez-Valera et al., 1982). Further studies revealed that halocin H4 is encoded by *halH4* gene, located on pHM300 plasmid, and the mature protein has a molecular weight of 34.9 kDa (Cheung et al., 1997; Rodriguez-Valera et al., 1982). Unexpectedly, in recent years, it was found that a *H. mediterranei* ATCC 33500 knockout mutant for *halH4* retained the inhibitory activity against *H. salinarum* and *H. volcanii* (Naor et al., 2013), proving that HalH4 is not responsible for its anti-haloarchaea activity.

Recently, lanthipeptides, a type of RiPP, were identified in the genomes of several haloarchaea by genome mining tools (Costa, 2017; Walker et al., 2020). Their possible involvement in the inhibitory activity of *H. mediterranei* ATCC 33500 was investigated (REF). Similar to halocin H4, knockout mutants for the *lanM* genes, the main genes involved in lanthipeptides biosynthetic pathway, retained the ability to inhibit other haloarchaea, confirming that lanthipeptides were not responsible for *H. mediterranei* activity (Castro, 2019). Therefore, it is still not clear which is the compound that allows *H. mediterranei* to inhibit other haloarchaea.

The antimicrobial activity of *H. mediterranei* ATCC 33500 has been characterized mainly in agar media and it is very reduced, or even absent, in broth. However, the production of biomass has been evaluated exclusively in broth media. To understand if haloazolisin's BGC might be involved in *H. mediterranei* anti-haloarchaea's bioactivity, it is important to understand if its genes are being transcribed or if they are silenced.

Thus, the first objective of this chapter was to monitor *H. mediterranei* WR510 (*H. mediterranei* Δ*pyrE*; section 3.1) growth and antimicrobial activity progression during five days on YPC-agar plates. The second objective was to quantify the transcription of *haloA* and *ycaO* under the same growth condition.

2.2. Materials and Methods

2.2.1. Strains, Medium, and Culture Conditions

H. mediterranei WR510 and *H. volcanii* H33 (Table 5) were routinely grown in YPC-agar medium at, respectively, 37°C for 5 days and 45°C for 5 days (or 37°C for 7 days). *H. mediterranei* WR510 is a derivative of ATCC 33500 strain (see section 3.1). *H. salinarum* NRC-1 (Table 5) was routinely grown in YPCss-agar medium at 37°C for 7 days. The plates were stored and conserved at 4°C. All growth media are described in TableS1.

2.2.2. Characterization of *H. mediterranei* WR510 growth and antimicrobial activity

An assay was designed in order to study the *H. mediterranei* WR510 growth and antimicrobial activity in YPC agar along 5 days (Figure 18). Briefly, liquid cultures of *H. mediterranei* WR510 were prepared and inoculated in the centre of YPC-agar plates in order to form of a "dot". The plates were incubated at 37°C for 5 days (120 hours). Every day, three plates were taken: i) one was used for viable cell counting by determining the number of colony forming units/mL (CFU/mL) and ii) the other two were treated 15 min with UV light and stored at 4°C. At day 5, the plates stored at 4ºC were used to test *H. mediterranei* antimicrobial activity against the indicator strains.

The following sections will describe in more detail each phase of this assay.

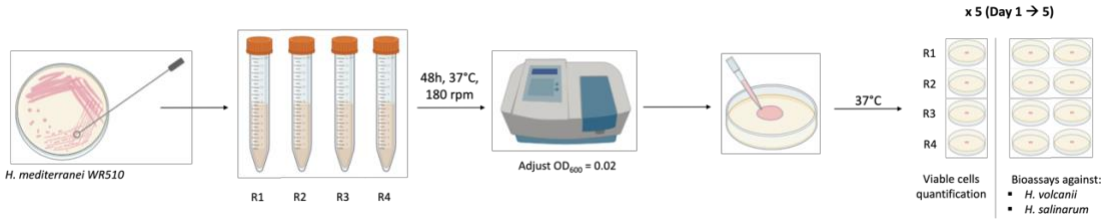

Figure 18. Schematic representation of the assay applied to evaluate *Haloferax mediterranei* WR510 growth and antimicrobial activity.

2.2.2.1. Preparation of cultures and plate inoculation

A fresh culture of *H. mediterranei* WR510 was used to inoculate 5-6 mL of YPC broth that were incubated at 37°C for 48h, with aeration (180 rpm). Their optical density at 600 nm (OD_{600}) was adjusted to 0.02 and 25 μL of this culture were plated in the form of a "dot" in the centre of YPC-agar plates (Figure 18) that were incubated at 37°C for 5 days. Four biological replicates were performed (Figure 18).

2.2.2.2. Growth monitoring

One plate for each biological replicate was collected every day and the number of viable cells in the dot biomass was quantified using an adaptation of the single plate-serial dilution spotting protocol (Thomas, Sekhar, Upreti, Mujawar, & Pasha, 2015).

Four mL of YPC broth were dispensed in the plate and used to completely dissolve the *H. mediterranei* biomass. The media was collected and its OD_{600} was measured and adjusted to 0.05. Then, serial decimal dilutions were prepared until $1x10^{-6}$ in a final volume of 1 mL of YPC broth. 20 μL of each dilution were dispensed in a YPC agar plate in the form of six micro-drops and in its correspondent sector, as shown in Figure 19. The plates were incubated at 37°C for 5 days and, after that, colonies were counted using the most appropriated dilution and the number of CFUs/mL determined.

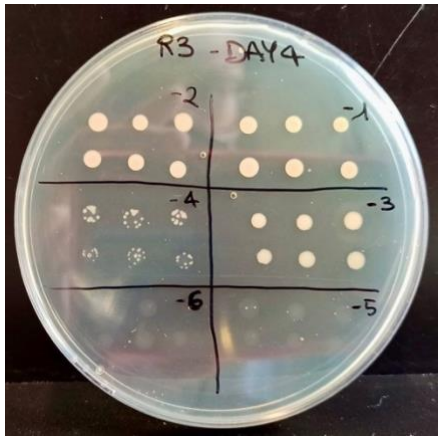

Figure 19. Example of a plate showing how the dilutions are dispensed in agar plates in the single plate-serial dilution spotting protocol.

2.2.2.3. Bioassays against other haloarchaea

Two plates of each biological replicate were collected every day, treated with UV light for 15 minutes and conserved at 4°C. At day 5, all the plates were used for overlay bioassay with *H. salinarum* and *H. volcanii*. For this, the two strains were grown in liquid culture (section 2.2.1) for 7 and 5 days, respectively. The OD_{600} of the cultures were measured and added to 15 mL of the respective soft-agar (TableS1), at a final OD_{600} = 0.03. Each indicator culture was then poured on the *H. mediterranei* plate and incubated at 37°C until the halo of inhibition was clearly visible for measuring.

2.2.3. Absolute quantification of gene transcription by qPCR

The expression of *ycaO* and *haloA* by *H. mediterranei* WR510 grown in YPC agar was determined by absolute quantification by real-time qPCR (RT-qPCR). First, RNA was

extracted from a suspension of *H. mediterranei* WR510 cells grown in agar and treated with DNases in order to avoid DNA contamination. After that, complementary DNA (cDNA) of the transcripts were synthesized and used for quantification by RT-qPCR (Figure 20).

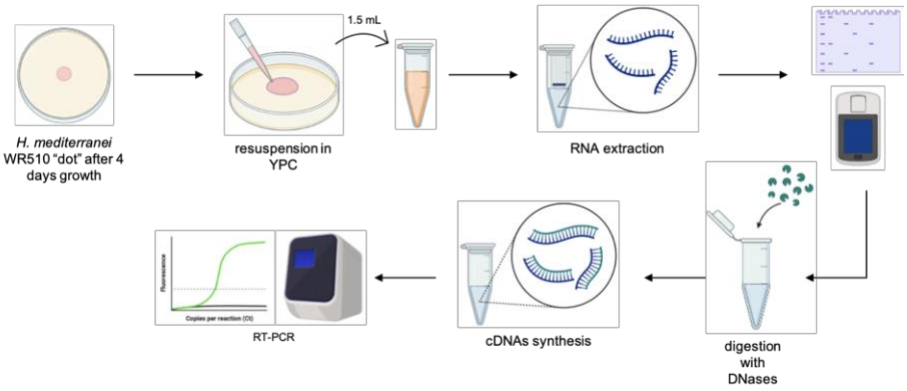

Figure 20. Schematic representation of the general protocol used to perform the quantification of gene expression in *H. mediterranei* by RT-qPCR.

2.2.3.1. RNA extraction

RNA was extracted from *H. mediterranei* WR510 cells grown in agar medium. The plates were prepared as described in section 2.2.2.1, in triplicate, and were incubated at 37°C for 4 days. Since it is not clear if the increment of the inhibitory activity is due to an actual increase of the antimicrobial compounds' concentration or to an increase of their diffusion, we decided to perform RNA extraction after 4 days, when the activity was clearly detectable and stable (section 2.3.2).

Four mL of YPC broth were dispensed in the plate and used to completely dissolve the *H. mediterranei* biomass. The cell suspension was collected and its OD_{600} was measured, adjusted to 0.5 and 1 mL was used for RNA extraction with the Quick-RNA MiniPrep Kit (Zymo Research), according to the manufacturer's instructions.

The integrity of the RNA was verified by electrophoresis with 1% agarose gel containing 1% of bleach. RNA concentration was determined with the fluorometer Qubit (Invitrogen).

2.2.3.2. cDNAs synthesis

Before cDNA synthesis, the extracted RNA was digested with DNases to eliminate any DNA contamination. Each reaction contained 1μL of ezDNase enzyme (Thermo Fisher), 1μL of 10X ezDNase buffer, 1μg of RNA and nuclease-free water up to a final volume of 10μL. The reactions were incubated at 37°C for 5 minutes. cDNA was synthesized by adding 4μL of SuperScript IV VILO Master Mix (Thermo Fisher) and 6μL of nuclease-free

water to each digestion, followed by incubation at 25°C for 10 minutes, then at 50°C for 10 minutes and, in the end, at 85°C for 5 minutes. In the end, 20μL of cDNA was obtained with a concentration of 50 ng/μL.

To completely exclude any total DNA contamination, the obtained cDNAs were tested in a PCR reaction with primers that annealed to sequences in two different transcriptional units, hence transcripts. Therefore, these primers would amplificate only in case of total DNA contamination.

Each PCR reaction was performed in a final volume of 12.5 μL, containing 0.75 μL of 50 mM $MgCl_2$ (NZYTech), 0.25 μL of 10 mM dNTPs (NZYTech), 2.5 μL of 5X Gel Load Reaction Buffer, 0.375 μL of forward primer (10 pmol/μL), 0.375 μL of reverse primer (10 pmol/μL), 1 μL of DNA template, corresponding to the synthesized cDNAs. Amplification parameters are listed in Table 3 and PCR products were run in an electrophoresis gel (1% agarose) at 120V for 45 minutes.

Table 3. Amplification parameters for PCR reaction to test cDNAs purity.

Target	Primers	Amplicon size	Steps	Temperature and Time	Cycles
ycaO	ycaO_UP_FW ycaO_DOWN_RV	2,503 bp/ 1,548 bp	Initial denaturation	95°C – 3’	-
			Denaturation	95°C – 30’’	
			Annealing	**60°C** – 30’’	30
			Extension	72°C – 1’15’’	
			Final extension	72°C – 5’	-

2.2.3.3. RT-qPCR

In order to understand if *ycaO* and *haloA* genes are being transcribed when *H. mediterranei* is grown in YPC agar, the cDNA obtained in section 2.2.3.2 was analysed using RT-qPCR. The analysis also included the gene *rpl16*, that encodes 50S ribosomal protein L16, and was used as reference gene.

Each qPCR reaction was performed in the final volume of 10 μL, containing 5μL of 2X PowerUp SYBR Green Master Mix (Thermo Fisher), 3 μL of nuclease-free water, 0.5 μL of forward primer (10 pmol/μL; Table 1), 0.5 μL of reverse primer (10 pmol/μL; Table 1) and 1 μL of template DNA. For the quantification standard curve, decimal serial dilutions of *H. mediterranei* WR510 total DNA (extracted as described at section 3.2.3) containing $1x10^5$ to $1x10^1$ copy/μL of the target gene was used as template DNA. For quantification of transcription, cDNA at a concentration of 10 ng/μL was used as template DNA. The amplification parameters are shown in Table 4 and a melt curve was obtained, after the last

extension step, by amplicon incubation at the temperature range of 65 °C – 95 °C, for 10 seconds, with increments of 0.5 °C.

Table 4. Amplification parameters for *ycaO*, *haloA* and *rpl16* RT-PCR.

Target	Primers	Amplicon size	Steps	Temperature and Time	Cycles
ycaO	check_ycaO_qPCR_Fw check_ycaO_qPCR_Rv	108 bp	UDG activation Dual-Lock DNAPol Denaturation Annealing/Extension	50°C – 2' 95°C – 2' 95°C – 3'' 60°C – 30''	- - 50
haloA	qPCR_2sdtry_haloA_fw qPCR_2sdtry_haloA_rv	140 bp	UDG activation Dual-Lock DNAPol Denaturation Annealing/Extension	50°C – 2' 95°C – 2' 95°C – 3'' 60°C – 30''	- - 50
rpl16	qPCR_rpl16s1_F qPCR_rpl16s1_R	86 bp	UDG activation Dual-Lock DNAPol Denaturation Annealing/Extension	50°C – 2' 95°C – 2' 95°C – 3'' 60°C – 30''	- - 50

2.3. Results and Discussion

2.3.1. Viable cell counts

In order to obtain a growth curve that could characterize the *H. mediterranei* WR510 culture in YPC agar plates (conditions used for antimicrobial assays), over time, the number of CFU/mL were determined along 5 days (120 hours) using the single plate-serial dilution spotting protocol (Thomas et al., 2015). This protocol was applied for the first time to *H. mediterranei* WR510 and the dilution of $1x10^{-4}$ was identified as the most appropriate to CFU counting (Figure 19).

The growth curve obtained (Figure 21) showed that the number of viable cells increased exponentially within the first 48h ($8.13x10^{7}\pm5.44x10^{6}$ CFUs/mL). In the following three days the number of viable cells stabilizes until reaching $2.31x10^{8}\pm5.31x10^{7}$ CFUs/mL. Since *H. mediterranei* WR510 cultivated in YPC broth reaches the stationary phase after 32h of growth (Castro, 2019), it takes more time to reach stationary phase when cultivated in YPC-agar.

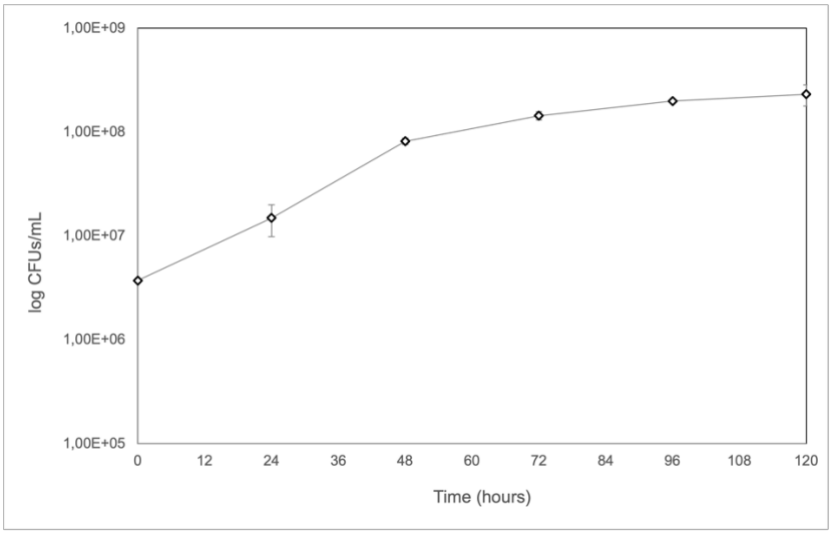

Figure 21. Growth curve of *Haloferax mediterranei* WR510 grown in YPC agar, at 37 ºC for 5 days.

2.3.2. Anti-haloarchaea activity of *H. mediterranei* WR510 along the time

The inhibition halos became distinctly visible for both indicator strains after 7 days of incubation at 37 ºC. The first noticeable difference between the indicators' plates was the type of the inhibition halo: the plates covered with *H. volcanii* showed a smeared inhibitory area whereas those covered with *H. salinarum* had a well-defined and detectable halo (Figure 22).

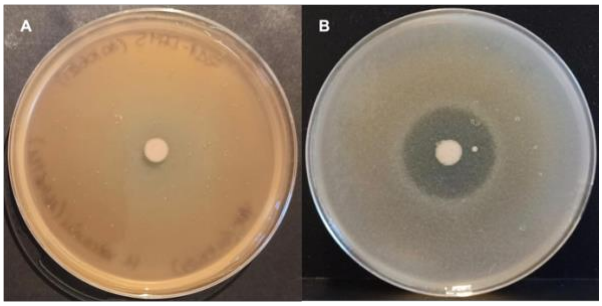

Figure 22. Inhibitory halos of *H. mediterranei* WR510 with 5 days of growth against *H. volcanii* (A) and *H. salinarum* (B).

The halos were measured to understand the progression of the antimicrobial activity along the 5 days (Figure 23, Figure 24). In the first 24 hours, no inhibition was evident against neither of the indicator strains (Figure 23). Then, the inhibitory activity strongly increased between the 24 and 96 hours (Figure 23) and, in the end, it stabilized between 96h and 120h (Figure 23).

In the last two days, the progression slowed down, especially for *H. volcanii* (Figure 23). Nevertheless, and for both species, the biggest halos are obtained after 4 or 5 days of incubation at 37 ºC.

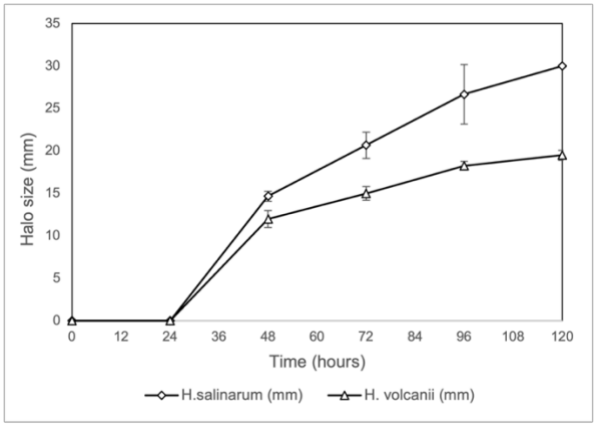

Figure 23. Inhibition halo produced by *Haloferax mediterranei* against the two indicator strains along five days. The y-axis reports the diameter of the halo (mm), while the x-axis reports the time (hours).

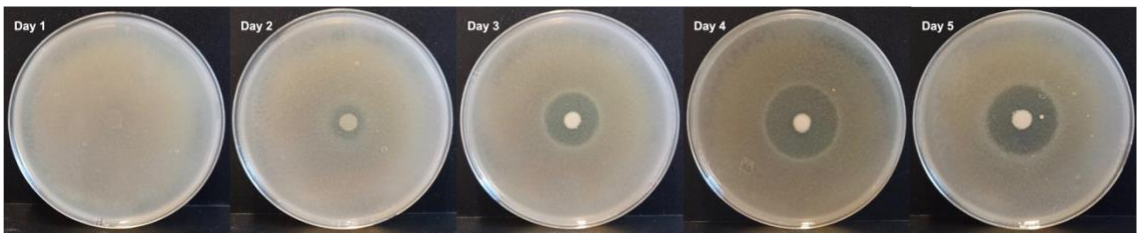

Figure 24. Progression of the inhibitory halo of *Haloferax mediterranei* against the indicator *Halobacterium salinarum* from day 1 to 5.

These results show an increase of the inhibitory activity along the 5 days, with a stabilization after 96 hours. With this kind of assays, it is unclear if the increase of inhibition corresponds to a higher concentration of the antimicrobial compounds, or if its results of a higher diffusion of the antimicrobial compounds over time.

Since the profile of the inhibitory activity seems to relate with the increase of biomass (Figure 21), the progression of the inhibition halo might be due to the actual increment of the antimicrobial compounds' concentration. Still, a bigger halo could just correspond to an increase of diffusion along time.

2.3.3. Quantification of *ycaO* and *haloA* transcription

Some secondary metabolite's BGCs are cryptic under certain laboratory conditions. In order to determine if haloazolisin BGC is cryptic in YPC agar, the medium used to study *H. mediterranei* anti-haloarchaea activity, the transcription of *ycaO* and *haloA* were analysed by RT-qPCR. This analysis allowed to quantify the level of gene transcription. However, to interpret the transcription levels obtained, the *rpl16* gene was also included in the analysis. This gene encodes a ribosomal protein and it has been used in other studies as internal control to perform relative quantification of gene expression by RT-qPCR (Fu et al., 2016; Hwang, Chavarria, Hackley, Schmid, & Maupin-Furlow, 2019).

The analysis was performed with RNA extracted after 4 days of growth in YPC agar since it corresponded to the time when the anti-haloarchaea activity of *H. mediterranei* towards both indicator strains have stabilized (as determined in section 2.3.2). As a general rule, RNA is extracted starting from liquid cultures, but in this specific situation our aim was to analyze *haloA* and *ycaO* transcription, which can vary depending on the culture medium, from agar-plate cultures.

Reaction efficiencies for *ycaO*, *haloA* and *rpl16* were 102.9%, 90.1% and 102.9% (Figure 25), respectively. All of them are within the acceptable range of 90-100%, allowing the quantification of all genes. It was concluded that both *ycaO* and *haloA* are expressed in *H. mediterranei* WR510 grown in YPC-agar in absence of any other microorganism. The detected number of gene copies/µL were $1.74x10^{3}\pm3.01x10^{2}$ for *ycaO* and $8.10x10^{1}\pm2.30x10^{1}$ for *haloA* (Figure 26).

It was concluded that *ycaO* was almost as expressed as *rpl16* ($5.97x10^{3}\pm1.26x10^{3}$ copies/µL), while *haloA* was about 100-fold less expressed than the two other genes (Figure 26). This difference between *ycaO* and *haloA* transcriptional level raises questions on their involvement in the same biosynthetic pathway.

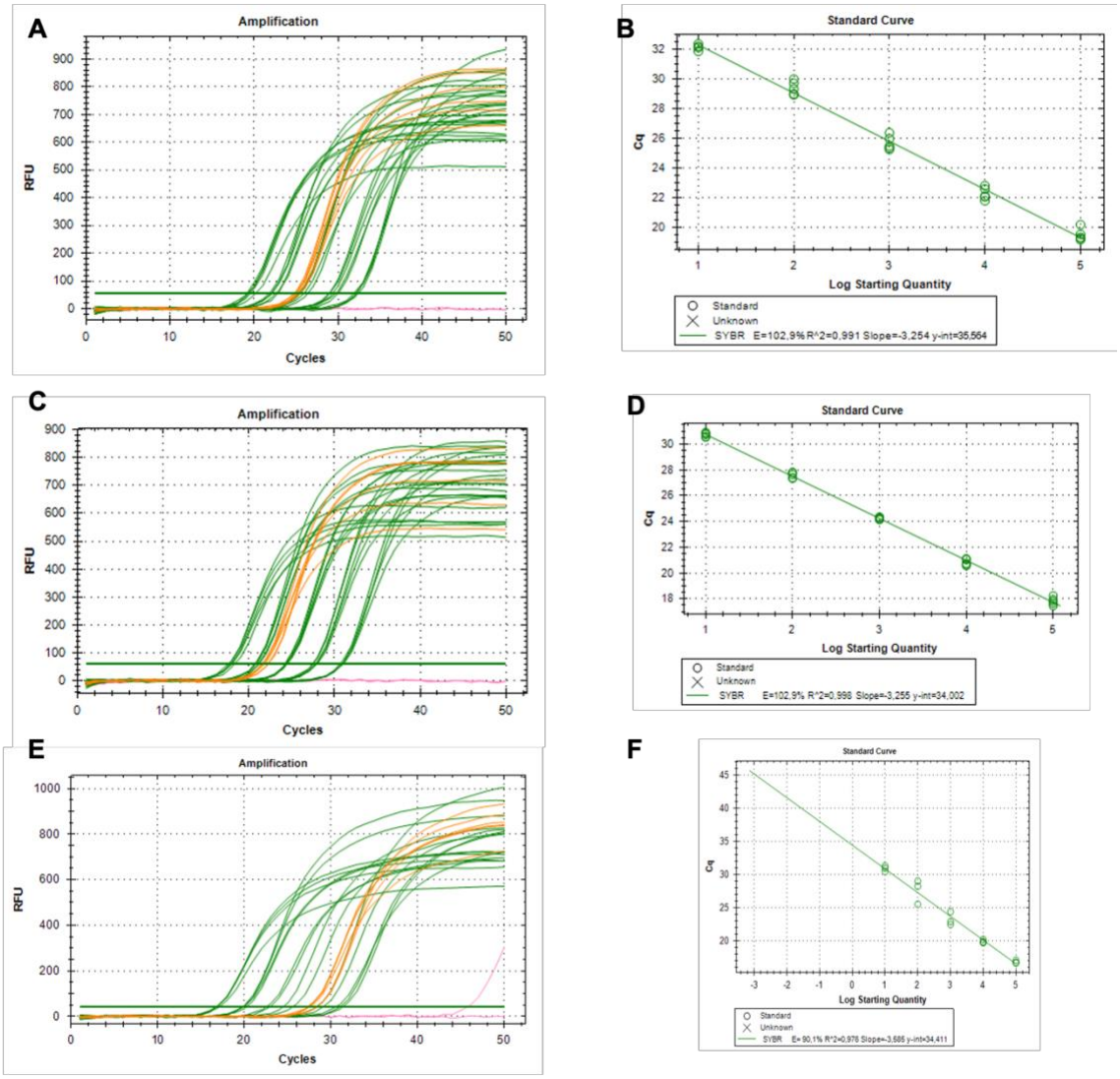

Figure 25. RT-PCR graphical results. In all images standards are reported in green, negative controls in pink and WR510 strain cDNA samples in orange. A, B) Amplification reaction and standard curve for *ycaO* quantification. C, D) Amplification reaction and standard curve for *rpl16* quantification. E, F) Amplification reaction and standard curve for *haloA* quantification.

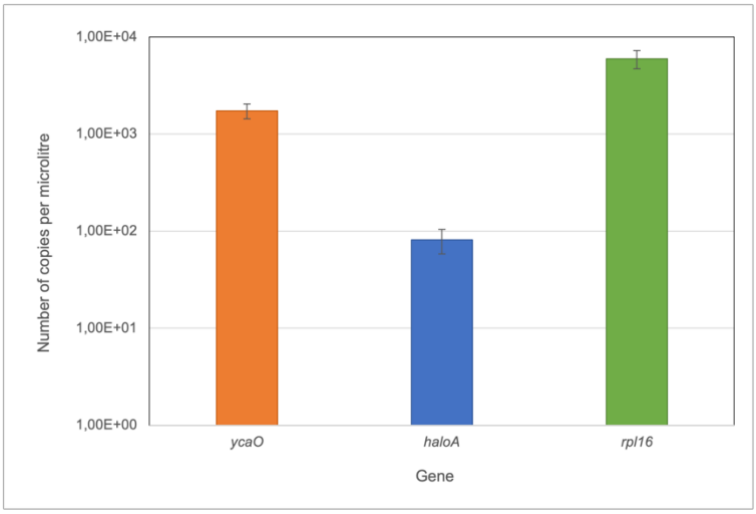

Figure 26. Results of absolute quantification of *ycaO*, *haloA* and *rpl16* transcription in *H. mediterranei* grown for 4 days in YPC agar at 37ºC.

2.4. Conclusions

The main conclusions of this chapter are:

i) The single plate-serial dilution spotting protocol was successfully adapted to *H. mediterranei* and can be used to quantify the number of viable cells in YPC-agar cultures;

ii) *H. mediterranei* inhibitory activity on agar-plate is undetectable after 24h, then increase progressively and stabilizes between 96h and 120h;

iii) It is not clear if, in YPC-agar, the increase of *H. mediterranei* inhibitory activity along the days is due to an increment of the antimicrobial compounds' concentration or to their diffusion;

iv) Gene *ycaO*, encoded by the haloazolin's BGC, is transcribed under the laboratory conditions used, being therefore not a cryptic gene; gene *haloA* is also transcribed, but at a lower extent than *ycaO* (almost less 100-fold), raising questions about their involvement in the same biosynthetic way.

3. Generation of knockout mutants

3.1. Introduction

One of the objectives of this study was to understand if the haloazolisin gene cluster identified in *H. mediterranei* ATCC 33500 (Figure 17) contributed to its antimicrobial activity by testing knockout mutants. The haloazolisin cluster is characterized by the gene *ycaO*, encoding the YcaO-like protein. This protein is putatively involved in the post-translational modification of a precursor peptide presumably encoded upstream of *ycaO* that was designated as *haloA* (Figure 17). Thus, these two genes were selected to generate knockout mutants that would not produce haloazolisin for further antimicrobial bioassays.

For this purpose, the *H. mediterranei* WR510 strain was used since it is a *H. mediterranei* ATCC 33500 strain that lacks the *pyrE* gene (Naor et al., 2013), which is involved in uracil biosynthetic pathway, and it can be used as selection marker during genetic manipulation procedures. *H. mediterranei* has been used as a model organism in studies regarding haloarchaea (Zuo et al., 2018) since its whole genome sequence is available and its genetic manipulation has already been well-established, as mentioned in section 1.2.1.

One of such procedures is the pop-in/pop-out strategy (Allers, Ngo, Mevarech, & Lloyd, 2004), that is a multistep technique allowing the generation knockout mutants based on the use of a recombinant plasmid that must contain only flanking regions and the beginning and the end of the target gene, but not the full gene to be further deleted (Figure 27). Thus, this technique consists of two main steps: i) promotion of the recombinant plasmid (also designated as knockout plasmid) integration into the gene to be deleted in the organism of interest (pop-in strain) and ii) promotion of the plasmid's excision from the pop-in-mutants, originating the pop-out strains. In the second step, the intrachromosomal recombination can allow the wild-type gene to leave together with the knockout plasmid leading to the generation of a knockout mutant (Allers et al., 2004; Bitan-Banin, Ortenberg, & Mevarech, 2003) (Figure 27). In this case, the target gene is substituted by its adjoining flanking sequences that were cloned into the multiple cloning site (MCS) of the recombinant plasmid. However, the intrachromosomal recombination can have other outcome, which is the exit of the original recombinant plasmid, leading to the maintaining of the wild-type gene (Allers et al., 2004; Bitan-Banin et al., 2003) (Figure 27).

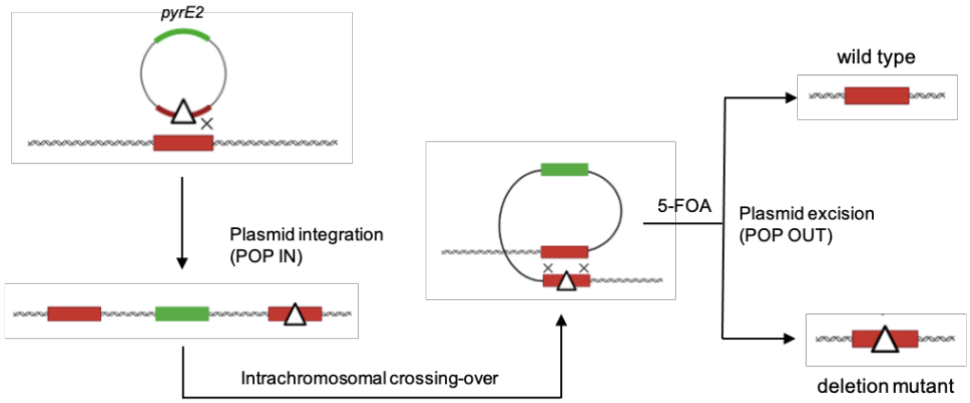

Figure 27. Representation of the genetic events involved in the pop-in/pop-out technique (adapted from Allers et al., 2004).

The vector of the knockout plasmid to be used in the pop-in/pop-out technique can´t have a haloarchaea's origin of replication and must carry the *pyrE2* gene, which is absent in *H. mediterranei* WR510, and is used as a pop-in selection marker (Bitan-Banin et al., 2003). Herein, the vector used was the pTA131 plasmid, which map is represented in Figure 28.

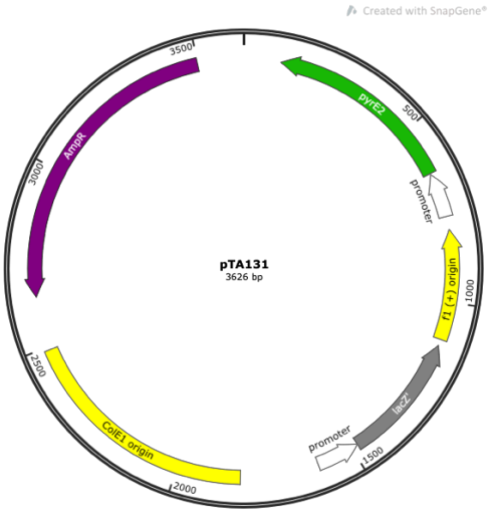

Figure 28. Map of the pTA131 plasmid. It contains a gene for ampicillin resistance (purple), the *pyrE2* gene from *Haloferax volcanii* (green), two origins of replication (yellow) and the *lacZ* gene (grey), with the MCS.

More specifically, the first step of the pop-in/pop-out technique is the transformation of WR510 strain with the knockout plasmid, followed by selection in casamino acids medium (CAM), which lacks uracil. In this media, the strains will be forced to use the orotate as precursor for dUTP biosynthesis (Figure 29). This pathway is dependent on the orotate phosphoribosyl transferase encoded by *pyrE* (Figure 29). Therefore, only the pop-in strains, that have integrated the plasmid in their genome (*pyrE*+), will be able to grow in CAM. Then,

these pop-in strains are grown in YPC medium (provides uracil) enriched with 5-fluoroorotic acid (5-FOA), in order to force the knockout plasmid excision and the generation of pop-outs. 5-FOA is an orotate analogue and, therefore, it is also a substrate of the orotate phosphoribosyl transferase. However, in the pyrimidine biosynthetic pathway, 5-FOA leads to the production of 5-fluoro-deoxyuridine triphosphate (5-FdUTP) that is a toxic compound causing the cell death (Figure 29). Therefore, this marker will force the excision of the plasmid by intrachromosomal crossing-over (Figure 27) in order to avoid the orotate pathway to produce dUTP and becoming pop-out strains lacking the *pyrE* gene. However, at this stage, and as abovementioned, the crossing-over can restore the wild-type genotype (wild-type pop-outs) or can result in a knockout mutant (pop-out mutants). Thus, to distinguish between wildtype and mutant pop-out strains, it is necessary to screen pop-out colonies by PCR and verify the size of the target gene.

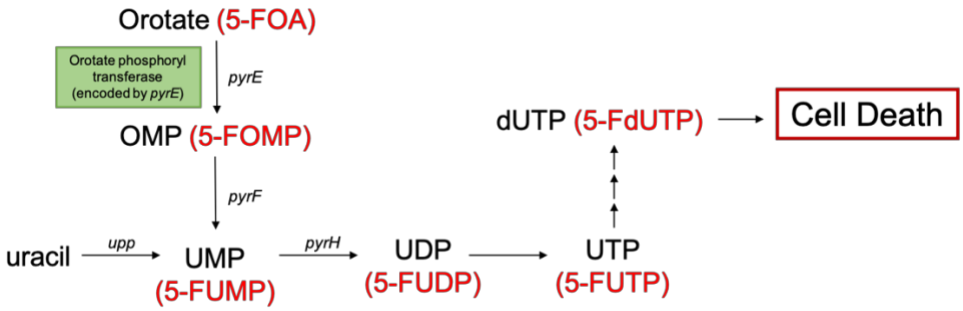

Figure 29. Representation of part of the dUTP biosynthetic pathway. 5-FOA is an orotate analogue and can serve as a substrate for the orotate phosphoryl transferase, leading to the formation of the toxic compound 5-FdUTP.

Afterwards, since *H. mediterranei* is a polyploid organism (section 1.2), the selected pop-out mutants need to be further tested to assure the absence of any copy of the target gene. This screening is ordinarily accomplished by southern blot (Allers et al., 2004) but herein RT-qPCR was used to amplify and quantify the deleted portion of the gene. This technique is less time consuming and easier compared to southern blot, but more important, it is extremely sensitive and would allow to detect very small quantities of gene copies whether they would be present.

The objective of this chapter was to obtain two mutants (*H. mediterranei ΔycaO* and *H. mediterranei ΔhaloA*), whose inhibitory activities will be tested in chapter 4.

3.2. Materials and Methods

3.2.1. Strains, Medium, and Culture Conditions

H. mediterranei WR510, *H. mediterranei* Δ*ycaO* and *H. mediterranei* Δ*haloA* (Table 5) were routinely grown in YPC-agar medium (TableS1) at 37°C for 5 days. The plates were stored and conserved at 4°C.

For *H. mediterranei* transformation and pop-in-mutants selection, CAM broth and CAM-agar plates, respectively, were used (TableS1). For the pop-out-mutants selection, 5-fluorotic acid (5-FOA) was added to the cultivation medium. 5-FOA was initially diluted in dimethyl sulfoxide (DMSO) to a final concentration of 10 mg/mL; this solution was then added to the YPC medium to reach a final concentration of 250 μg/mL.

For the recombinant plasmid construction, *Escherichia coli* competent cells NZY5α (NZYTech) were used. They were grown in Luria Bertani broth (LB; Liofilchem) and Luria Bertani agar (LA; NZYTech). *Escherichia coli* containing pTA131 were conserved in glycerol (400 μl liquid culture + 200 μl glycerol 45%) at -80°C and reactivated when necessary.

Table 5. Strains and plasmids used in this work.

Name	Properties	Reference
Haloferax mediterranei WR510	Δ*pyrE*	(Naor et al., 2013)
Haloferax mediterranei Δ*ycaO*	Δ*pyrE,* Δ*ycaO*	This study
Haloferax mediterranei Δ*haloA*	Δ*pyrE,* Δ*haloA*	This study
Haloferax volcanii H33	Δ*pyrE,* Δ*trpA*	(Allers et al., 2004)
Halobacterium salinarum NRC-1	wild-type	(Naor et al., 2013)
Escherichia coli NZY5a	Competent cells	NZY Tech
pTA131	*pyrE*$^+$, *lacZ*$^+$, amp resistance	(Allers et al., 2004)
pKO_ycaO	*pyrE*$^+$, amp resistance, containing *ycaO* flanking sequences	This study
pKO_haloA	*pyrE*$^+$, amp resistance, containing *haloA* flanking sequences	This study

3.2.2. Plasmid extraction

For pTA131 extraction, *E. coli* cells containing pTA131 were cultivated in LB medium supplemented with Amp 50 μg/mL, overnight at 37ºC with agitation (180 rpm). The culture was then used to extract plasmid DNA with the NZYMiniPrep Kit (NZY Tech), according to the manufacturer's instructions. The same procedure was used to extract the plasmids constructed in this study (pKO_ycaO and pKO_haloA; described in section 3.2.4).

3.2.3. Total DNA extraction

H. mediterranei WR510 was inoculated from an YPC agar plate into 5mL of YPC broth and incubated at 37ºc with agitation at 180 rpm for 48h. 1 mL of this culture was used to extract total DNA with the protocol for Gram negative bacteria of the Wizard Genomic DNA Purification Kit (Promega), according to the manufacturer's instructions. The same procedure was applied to extract DNA from *H. mediterranei* Δ*ycaO* and Δ*haloA* mutants.

3.2.4. Construction of knockout plasmids

Two recombinant knockout plasmids, namely pKO_ycaO and pKO_haloA (Table 5), were constructed to delete *ycaO* and *haloA* genes, respectively, from *H. mediterranei* WR510 genome. Each knock-out plasmid was constructed by the insertion of two fragments of about 800 bp, corresponding to the flanking sequences of the target gene, into the *lacZ* gene of plasmid pTA131 (MCS; Figure 30).

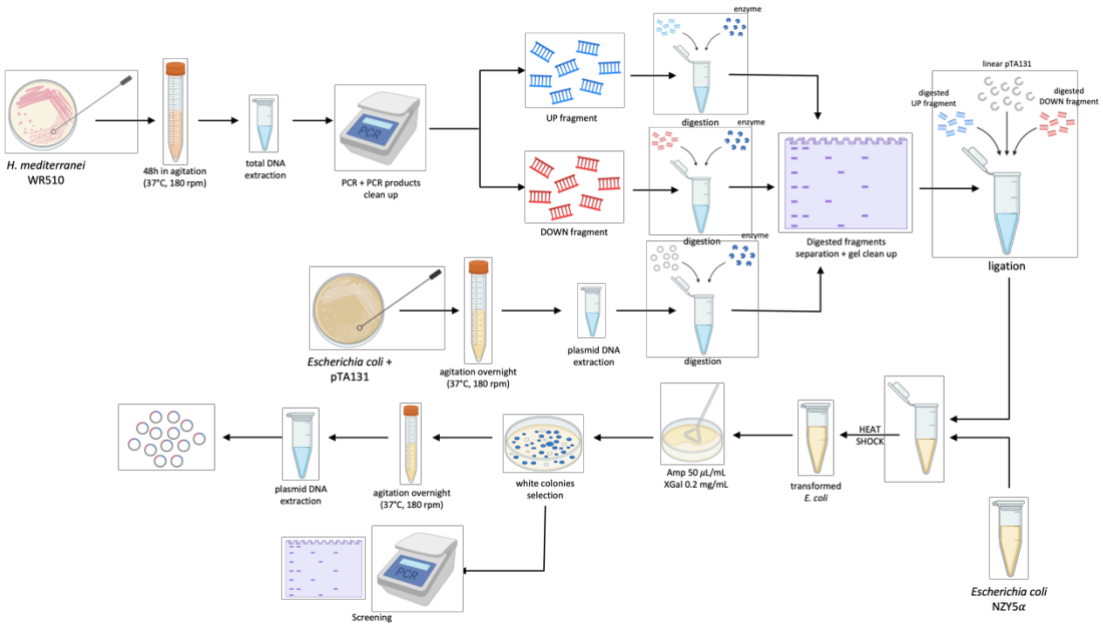

Figure 30. Schematic summary of the recombinant plasmids' construction.

3.2.4.1. Amplification of fragments

For the amplification of upstream (up) and downstream (down) fragments of the target gene, primers (TableS2) were designed with the software Primer 3 (Untergasser et al., 2012) following the rational shown in Figure 31. Restriction sites were added to the primers according to TableS2.

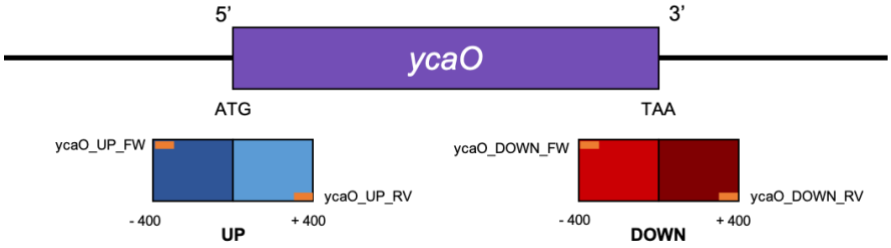

Figure 31. Primers design representation for *ycaO* gene. Primers (orange) were designed to amplify two fragments of about 800 bp each, including part of the gene (light blue and light red) and its flanking sequences (dark blue and dark red). The same approach was used for *haloA* gene.

The amplification of each fragment was performed in three separated PCR reactions of a final volume of 50 μL that were then put together. Each PCR reaction contained 0.5 μL of DNA template (52 ng/μL), 2.5 μL of forward primer (10 pmol/μL), 2.5 μL of reverse primer (10 pmol/μL), 25 μL of 2X Platinum SuperFi PCR Master Mix (Thermo Scientific) and 19.5 μL of nuclease free water. Total DNA extracted from *H. mediterranei* WR510 (section 3.2.3) was used as DNA template and the amplification parameters for each fragment are listed in Table 6. The success of the amplification was verified by agarose gel electrophoresis (1.0%) and the amplicons were purified using the protocol for PCR clean-up of the GelPure Kit (NZYTech), according to manufacturer's instructions.

Table 6. Amplification parameters used for each fragment. The primers used in these reactions are listed in TableS2.

Target	Primers	Amplicon size	Amplification steps	Temperature and Time	Cycles
ycaO up region	ycaO_UP_FW ycaO_UP_RV	805 bp	Initial denaturation	98°C – 30''	-
			Denaturation	98°C – 10''	
ycaO down region	ycaO_DOWN_FW ycaO_DOWN_RV	780 bp	Annealing	**69°C** – 10''	30
			Extension	72°C – 30''	
haloA down region	ycaO_DOWN_FW ycaO_DOWN_RV	776 bp	Final extension	72°C – 5'	-
haloA up region	ycaO_UP_FW ycaO_UP_RV	814 bp	Initial denaturation	98°C – 30''	-
			Denaturation	98°C – 10''	
			Annealing	**60°C** – 10''	30
			Extension	72°C – 30''	
			Final extension	72°C – 5'	-

3.2.4.2. Digestion with restriction enzymes

Each fragment and pTA131 were digested in separated reactions with the respective restriction enzymes (TableS2). Since plasmid pTA131 was needed for both knockout

plasmids' construction, it was digested into two separated reactions with different restriction enzymes. Namely, for pKO_ycaO construction, pTA131 was digested with *Bam*HI and *Xba*I, while for pKO_haloA construction, pTA131 was digested with *Bam*HI and *Kpn*I.

The total volume of each digestion reaction was 20 μL containing 2μL of 10X Buffer, 1μL of each of the two restriction enzymes and 1μg of DNA to digest (either the PCR fragments or pTA131 plasmid). Digestions used for the construction of pKO_ycaO and pKO_haloA plasmids were performed with the Anza restriction enzymes (Thermo Scientific) and with FastDigest restriction enzymes (Thermo Scientific), respectively. The reactions were incubated at 37°C for 20 minutes, loaded on an electrophoresis agarose gel (1.0%) and runned at 120V for 45 minutes. Each digestion product was excised from the gel and DNA was purified with the GelPure Kit (NZYTech), according to manufacturer's instructions.

3.2.4.3. Ligation and transformation

In order to obtain the two knockout plasmids, two ligation reactions were performed separately. The total volume of each reaction was 20 μL, containing 5 μL of Anza T4 DNA Ligase Master Mix (Thermo Scientific), 50 ng of digested vector, 40 ng of digested up fragment and 40 ng of digested down fragment. The two ligation reactions were incubated at 37°C for 20 minutes and 5 μL were used to transform 50 μL of *E. coli* NZY5α competent cells (NZYTech) by heat shock approach. Specifically, this mixture was incubated on ice for 10 minutes, transferred to 42°C for 45 seconds and immediately placed on ice again for 2 minutes. After that, 945 μL of LB were added to the cells and the culture was left in agitation at 37°C, 180 rpm, for 1 hour. The cells were collected by centrifugation at 5,000 rpm for 1 minute and the supernatant was discarded. The cell pellet was resuspended in the leftover supernatant and plated with glass beads on LA plates containing 50 μg/mL Amp and 0.2 mg/mL of XGal, and incubated overnight at 37°C. Since the vector contains the Amp resistance gene (Figure 28), only transformed colonies were able to grow in this selective medium. XGal allowed to discriminate between *E. coli* that integrated the wild-type plasmid (blue colonies), and those that integrated the recombinant plasmid (white colonies).

Screening of white colonies was performed by colony PCR to confirm the presence of both upstream and downstream fragments using universal primers that target the flanking regions of *lacZ* gene (TableS2) and PCR products were loaded on an electrophoresis agarose gel (1.0%) to estimate the amplicon size. The expected amplicon size for colonies containing the recombinant plasmid was about 1900 bp, corresponding to the *lacZ* gene with the insertion of both up and down fragments. Colony-PCR reactions had a final volume of 12.5 μL, containing 0.6 μL of forward primer (10 pmol/μL), 0.6 μL of reverse primer (10

pmol/μL), 6.3 μL of 2X Platinum SuperFi PCR Master Mix (Thermo Scientific) and the DNA template was biomass of a white colony. The amplification program applied is listed in Table 7. A positive colony was selected to extract pKO_ycaO and pKO_haloA plasmids as described in 3.2.2. The MCS region of both plasmids was sequenced at StabVida (Portugal).

Table 7. Amplification parameters for the screening of *E. coli* colonies.

Target	Primers	Amplicon size	Steps	Temperature and Time	Cycles
Flanking regions of *lacZ*	pUC19_FW pUC19_RV	301 bp (wild-type)/ ~1,900 bp (recombinant)	Initial denaturation	98°C – 30''	-
			Denaturation	98°C – 10''	
			Annealing	**54°C** – 10''	30
			Extension	72°C – 1'	
			Final extension	72°C – 5'	-

3.2.5. Generation of *Haloferax mediterranei* mutants

H. mediterranei was transformed with pKO_ycaO and pKO_haloA separately, using the transformation PEG-mediated protocol (Allers et al., 2004), in order to obtain two pop-in-mutants (Figure 32).

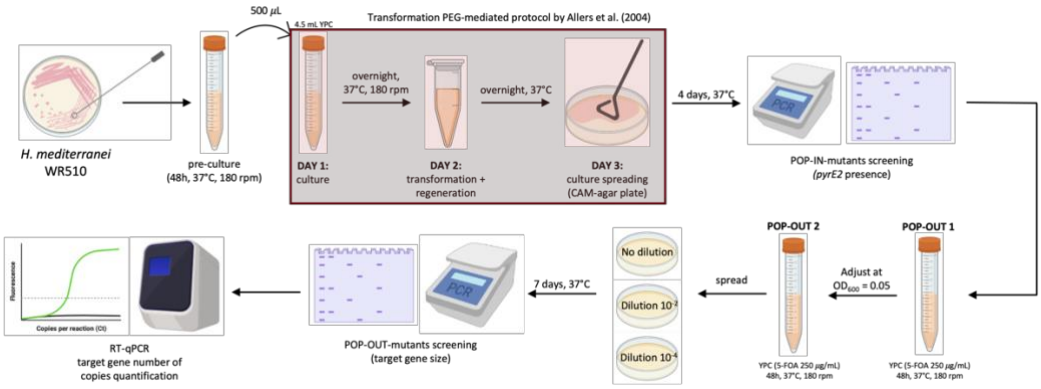

Figure 32. *Haloferax mediterranei* transformation and mutants' selection.

These were screened to test the presence of *pyrE2* gene, and the selected pop-in strains were grown in liquid cultures with 5-FOA, in order to force the plasmid exit (Figure 32). In the end, the pop-out-mutants were screened to confirm the absence of any copy of the deleted gene. This last step is very important because haloarchaea, including *H. mediterranei*, are polyploid (section 1.2), therefore pop-out-mutants could have conserved some copies of the gene somewhere on the genome.

3.2.5.1. Generation of pop-in strains

H. mediterranei WR510 was grown in YPC at 37 ºC, with aeration (180 rpm) until the OD_{600}>0.5. This culture was used for the transformation protocol with 1 μg of pKO_ycaO or pKO_haloA plasmids following the PEG-mediated protocol by Allers *et al.* (2004). The transformants were plated in CAM-agar plates and incubated at 37°C for 4 days. Several colonies were tested by colony-PCR to verify the presence of *pyrE2* gene. Each colony-PCR reaction was performed as described in section 3.2.4.3, with the primers and amplification program of Table 8. PCR products were analysed after agarose gel electrophoresis. One positive colony for each plasmid was selected to obtain pop-outs as described in the following section.

Table 8. Amplification parameters used in the screening of pop-in-mutants.

Target	Primers	Amplicon size	Steps	Temperature and Time	Cycles
pyrE2	pyrE2_haloferax_FW pyrE2_haloferax_RV	227 bp	Initial denaturation	98°C – 30''	-
			Denaturation	98°C – 10''	
			Annealing	**56°C** – 10''	30
			Extension	72°C – 30''	
			Final extension	72°C – 5'	-

3.2.5.2. Generation of pop-out mutants

In order to force the plasmid excision, one pop-in strain was grown in 10 mL of YPC supplemented with 5-FOA (see section 3.2.1) at 37ºC, for 2 days, with aeration (180 rpm). This culture was used to inoculate fresh medium with a final OD_{600} = 0.05 and grown in the same conditions for 2 more days. 50 μL of this culture and its dilutions (10^{-2} and 10^{-4}) were spread on YPC agar plates containing 5-FOA (250 μg/mL). The plates were incubated at 37 ºC and colonies were visible after one week. Plasmid excision can restore the wild-type genotype or can generate knockout mutants for the target gene. Thus, colonies were screened by colony-PCR to discriminate between these two possibilities and identify pop-out strains for screening.

For *H. mediterranei* Δ*ycaO* mutants screening, each colony-PCR reaction was performed as described in section 3.2.4.3, with the primers and amplification program of Table 9. PCR products were analysed after agarose gel electrophoresis.

Table 9. Amplification parameters used in the screening of ⊿ycaO pop-out-mutants.

Target	Primers	Amplicon size	Steps	Temperature and Time	Cycles
ycaO	ycaO_UP_FW ycaO_DOWN_RV	2,503 bp (wild-type)/ 1,548 bp (pop-out-mutants)	Initial denaturation Denaturation Annealing Extension Final extension	98°C – 30'' 98°C – 10'' 60°C – 10'' 72°C – 1'15'' 72°C – 5'	- 30 -

For *H. mediterranei ⊿haloA* mutants screening, each colony-PCR reaction was performed in a final volume of 12.5 μL, containing 0.75 μL of 50 mM $MgCl_2$ (NZYTech), 0.25 μL of 10 mM dNTPs (NZYTech), 2.5 μL of 5X Gel Load Reaction Buffer, 0.375 μL of forward primer (10 pmol/μL), 0.375 μL of reverse primer (10 pmol/μL), 1 μL of DNA template. DNA template was a suspension of colony biomass in 50 μL of distilled water. Amplification parameters of the PCR reaction are described in Table 10. PCR products were analysed after agarose gel (2%) electrophoresis.

Table 10. Amplification parameters for the screening of *⊿haloA* pop-out-mutants.

Target	Primers	Amplicon size	Steps	Temperature and Time	Cycles
haloA	haloA_UP_FW haloA_DOWN_RV	1,584 bp (wild-type)/ 1,557 bp (pop-out-mutants)	Initial denaturation Denaturation Annealing Extension Final extension	95°C – 3' 95°C – 30'' **60°C** – 30'' 72°C – 1' 72°C – 5'	- 30 -
haloA	check_UP_haloA check_haloA_qPCR_Rv	156 bp (wild-type)/ 129 bp (pop-out-mutants)	Initial denaturation Denaturation Annealing Extension Final extension	95°C – 3' 95°C – 30'' **60°C** – 30'' 72°C – 30'' 72°C – 5'	- 30 -

3.2.5.3. Confirmation of mutants by RT-qPCR

To confirm the total absence of the target genes in the selected mutants, RT-qPCR to quantify the copy number of each gene in selected pop-out mutants. Each RT-qPCR reaction was performed in a final volume of 10 μL, containing 5μL of 2X PowerUp SYBR Green Master Mix (Thermo Fisher), 0.5 μL of forward primer (10 pmol/μL), 0.5 μL of reverse primer (10 pmol/μL), and 1 μL DNA template. For the standard curve, DNA template corresponded to decimal serial dilutions of *H. mediterranei* WR510 total DNA that represented $1x10^5$ to 1 copy/μL of the target gene. The DNA template used for quantification

was total DNA of the mutants at a concentration of 10 μg/μL, extracted following the protocol described in section 3.2.3. The amplification program used is listed in Table 11. After the last extension step, a melt curve was obtained for temperature range between 65 °C and 95 °C, with an incubation time of 10 seconds for each increment of 0.5 °C.

The primers used for these quantification reactions are listed in TableS2 and were designed to amplify the region of each target gene that was deleted in the mutants. Hence, it was expected to obtain a quantification of 0 copies/μL in the mutants.

Table 11. Amplification parameters used for the quantification of the target gene number of copies in mutants.

Target	Primers	Amplicon size	Steps	Temperature and Time	Cycles
ycaO	check_ycaO_qPCR_Fw check_ycaO_qPCR_Rv	108 bp	UDG activation Dual-Lock DNAPol Denaturation Annealing/Extension	50°C – 2' 95°C – 2' 95°C – 3'' 60°C – 30''	- - 30
haloA	check_UP_haloA check_haloA_qPCR_Rv	156 bp (wild-type)/ 129 bp (pop-out-mutants)	UDG activation Dual-Lock DNAPol Denaturation Annealing/Extension	50°C – 2' 95°C – 2' 95°C – 3'' 60°C – 30''	- - 30

3.3. Results and Discussion

3.3.1. Construction of recombinant plasmids

The two recombinant plasmids pKO_ycaO and pKO_haloA (Figure 33) were obtained by cloning the flanking sequences of each target gene (respectively *ycaO* and *haloA*) into plasmid pTA131.

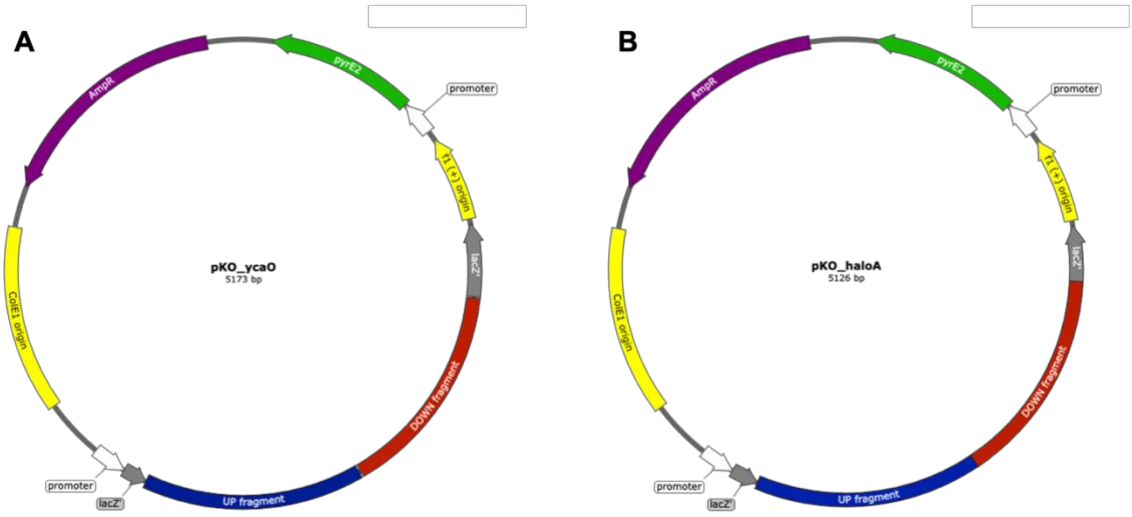

Figure 33. Maps of pKO_ycaO (A) and pKO_haloA (B) plasmids. They contain a gene for ampicillin resistance (purple), the *pyrE2* gene from *H. volcanii* (green), two origins of replication (yellow), and the interrupted *lacZ* gene (grey), where the UP (blue) and DOWN (red) fragments of the target gene were inserted.

For *ycaO* it was easy to design the most appropriated primers since there is not overlap with other genes. For *haloA*, it was possible to design primers only in a small and specific sequence, because it overlaps with another gene of unknown function, encoded in the opposite strand (Figure 17). Therefore, in order to maintain the other gene, primers were design to generate a *ΔhaloA* knockout that will miss the first amino acids of HaloA, and not the entire gene.

3.2.2. Selection of *H. mediterranei* Δ*ycaO* and Δ*haloA* pop-outs

After the pop-in and pop-out procedure, the *H. mediterranei* pop-out mutants were identified by colony-PCR (Figure 34), as described at section 3.2.5.2.

For *H. mediterranei* Δ*ycaO* mutants the expected amplicon size was 1,548 bp, while for the wild-type pop-out it was 2,503 bp. Twenty colonies were screened and ten of them were confirmed as pop-out mutants, corresponding to the 50% of the mutants.

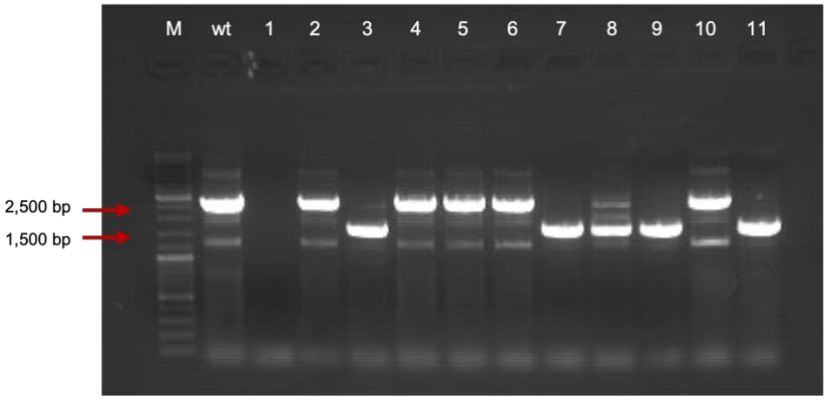

Figure 34. Agarose gel showing the result of the screnning of *ΔycaO* pop-out colonies by colony-PCR. Amplicons were separated in an 1% agarose gel at 120V for 45'. M corresponds to the GeneRuler DNA Ladder Mix (Thermo Fisher), and wt corresponds to WR510 strain. Colonies 3, 7, 9, and 11 were pop-out mutants.

Similarly, for *H. mediterranei* Δ*haloA* mutants the expected amplicon size was 1,557 bp, while for the wild-type pop-out was 1,584 bp. This amplicon was obtained by using the primers haloA_UP_FW and haloA_DOWN_RV (section 3.2.5.2 and TableS2), which were two of the four primers designed for the amplification of *halo*A UP and DOWN fragments. However, due to the small difference of size between the two fragments and to their molecular weight, it was not possible to distinguish the wild-type from the pop-out mutant colonies clearly (Figure 35A).

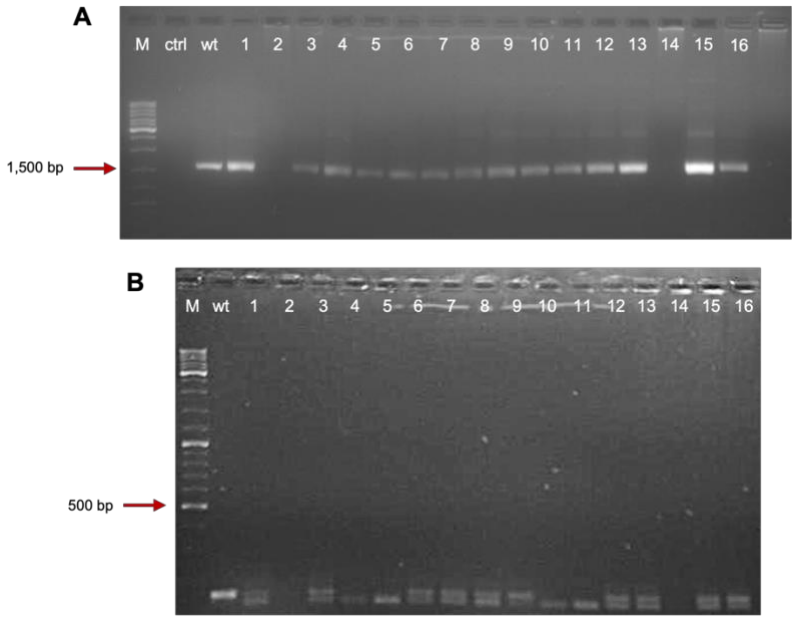

Figure 35. A) Electrophoresis gels for *ΔhaloA* mutants' screening (primers: haloA_UP_FW and haloA_DOWN_RV). Samples were run in an agarose 2% gel at 120V for 70'. B) Electrophoresis gels for *ΔhaloA* mutants' screening (Primers check_UP_haloA and check_haloA_qPCR_RV). Samples were run in an agarose 2% gel at 100V for 60'. Colonies 4, 5, 10, and 11 are pop-out-mutants. M corresponds to the GeneRuler DNA Ladder Mix (Thermo Fisher), ctrl is the negative control and wt corresponds to WR510 strain.

Therefore, a second PCR was performed with different primers (section 3.2.5.2 and TableS2) to amplify a smaller fragment of *halo*A gene. In this reaction, the expected amplicon sizes were 156 bp for the wild-type pop-outs and 129 bp for the pop-out mutants (Figure 35B). Forty colonies were screened and among them only six were identified as pop-out-mutants, corresponding to the 15% of the mutants.

3.2.3. Confirmation of pop-out mutants by RT-qPCR

The selected pop-out mutants were analysed by RT-qPCR, in order to verify the absence of copies of the target gene. Firstly, a standard curve for each target gene was obtained using known decimal serial dilutions from $1x10^5$ to 1 copy/µL of the target gene. Then, amplification of the target gene was performed with total DNA of the pop-out mutants to quantify the target gene copy number, as described at section 3.2.5.3.

3.2.3.1. RT-qPCR for *H. mediterranei ΔycaO* pop-out mutant

In order to quantify the *ycaO* copy number in *H. mediterranei ΔycaO* mutant, two primers were designed to amplify a region of the gene that was deleted.

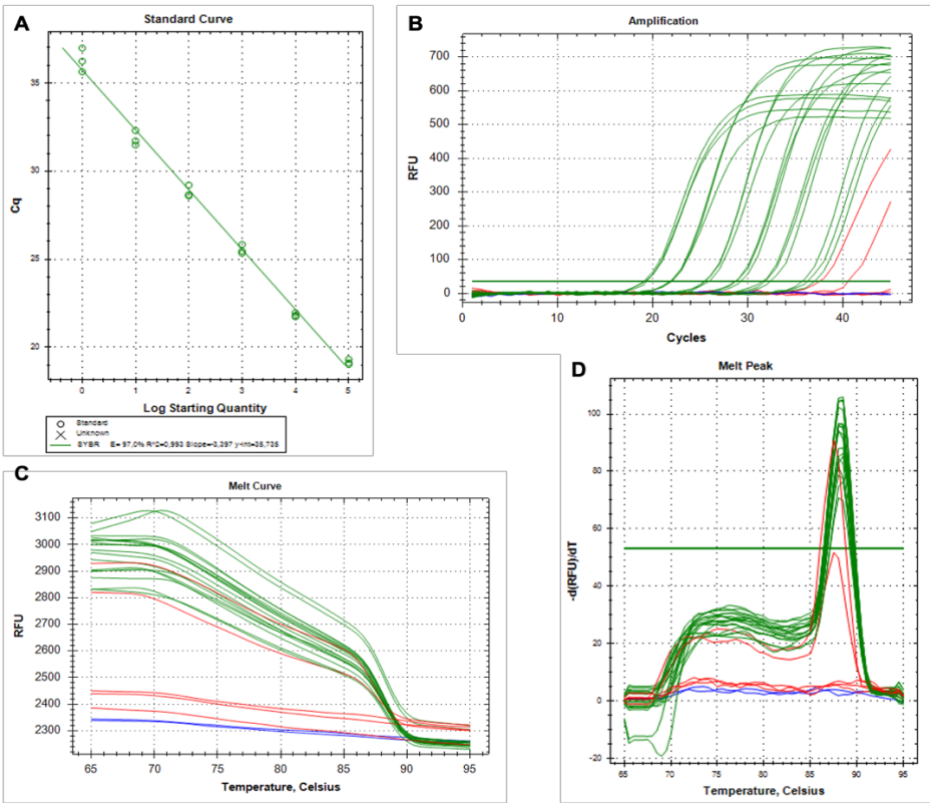

Figure 36. Results from RT-qPCR analysis of *H. mediterranei ΔycaO*, showing: A) the standard curve obtained for *ycaO* amplification (efficiency = 97.0%, R^2 = 0.993), B) the *ycaO* amplification curves, C) the melt curve of the amplicons and D) the melt peaks of amplicons. Green, red and blue lines represent the standard curve, the *ΔycaO* mutants and the negative controls reactions, respectively.

The RT-qPCR performed proved to be efficient (E = 97.0%; Figure 36A) and the negative controls showed no contamination (Figure 36B).

The three replicates of the *H. mediterranei ΔycaO* pop-out-mutant tested showed no amplification (Figure 36B), which confirmed the absence of *ycaO* in its genome. Two replicates showed amplification (Figure 36B), but below the detection limit established by the standard curve of 1 copy/µL. Also, the melt curve and corresponding melt peak (Figure 36C, Figure 36D) of the amplicons differ from those obtained with the *H. mediterranei* WR510 DNA in the standard curve, confirming that the amplified fragment can not represent the intact *ycaO* gene. Thus, the *H. mediterranei ΔycaO* tested was confirmed as a knockout mutant and used for further antimicrobial testing (Chapter 4). These results proved that qPCR can be used as a valid, and even more sensitive method than Southern blot, for gene copies detection.

3.2.3.2. RT-qPCR for *H. mediterranei ΔhaloA* pop-out mutant

In order to quantify the *haloA* copy number in *H. mediterranei ΔhaloA* mutant, two primers were designed to amplify a region of the gene that was deleted, as for *ycaO* gene. The *haloA* region deleted in *H. mediterranei ΔhaloA* consisted of only 27 bp (Figure 17), which have limited the primer design options. The RT-qPCR analysis showed a low efficiency (E<90%; Figure 37B) since amplification was obtained only for the $1x10^5$ and $1x10^4$ copies/µL standards and only after 25 cycles (Figure 37A). Therefore, it was necessary to design new primers and due to the small size of the *haloA* deleted region, another approach had to be adopted.

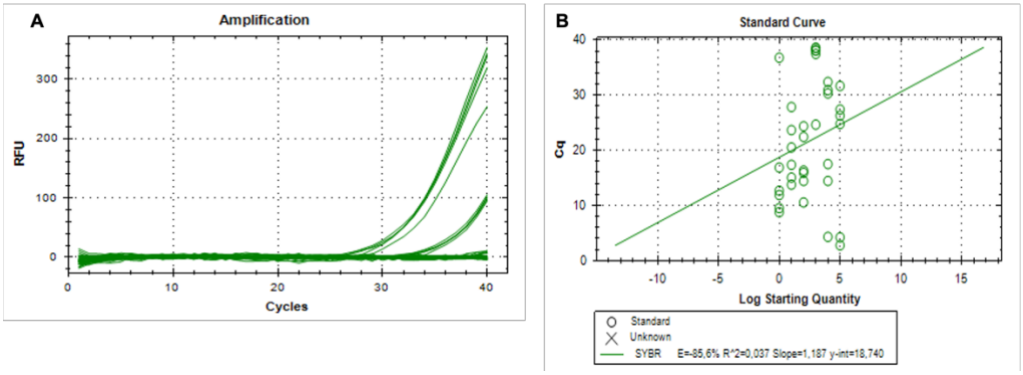

Figure 37. Results from RT-qPCR analysis of *H. mediterranei ΔhaloA*, showing: A) the *haloA* amplification curves, B) the standard curve obtained for *haloA* amplification (efficiency = 85.6%, R^2 = 0.037).

The novel approach implied the design of two primers to obtain an amplicon that included the deleted region. The rational was to confirm the knockout mutant throughout the analysis

of the amplicon's melt peak and not by gene copy quantification. Following this, the *ΔhaloA* knockout DNA was expected to originate one amplicon, with a lower molecular weight and consequently with a distinct melt peak from the wild-type amplicon.

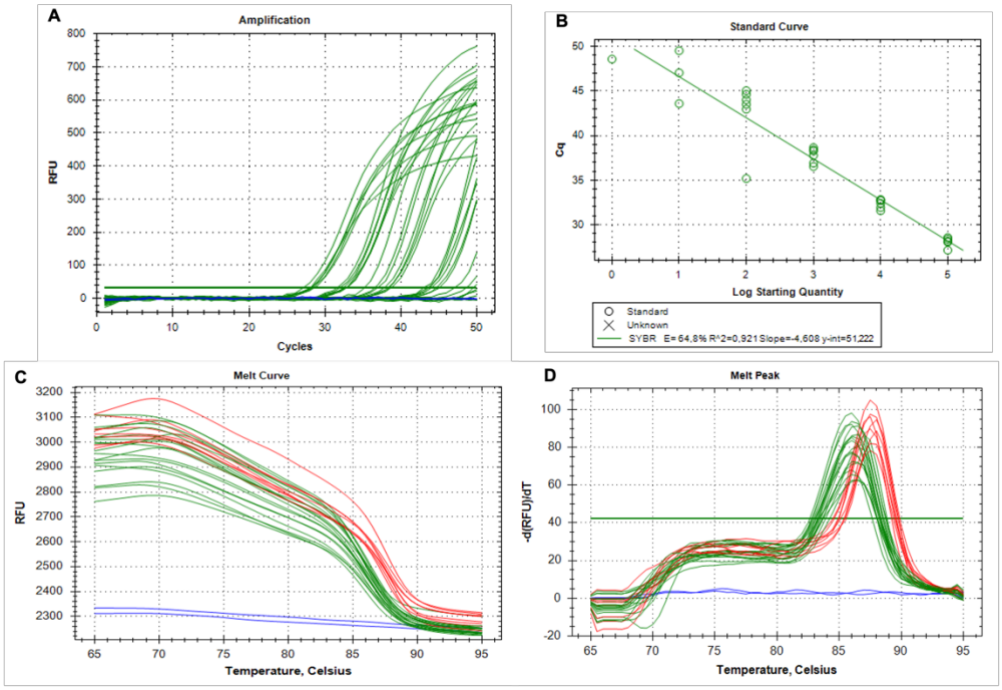

Figure 38. Results from RT-qPCR analysis of *H. mediterranei ΔhaloA*, showing: A) the *haloA* amplification curves, B) the standard curve obtained for *haloA* amplification (efficiency = 64.8%, R^2 = 0.921), C) the melt curve of the amplicons and D) the melt peaks of amplicons. Green, red and blue lines represent the standard curve, the *ΔhaloA* mutants and the negative controls reactions, respectively.

Again, the RT-qPCR analysis showed a low efficiency (E <90%; Figure 38A), but the negative controls showed no contamination (Figure 38A). Nevertheless, the two *ΔhaloA* colonies tested showed only one amplicon since only one melt peak was visible (Figure 38D), as expected. Also, these amplicons had a melting temperature of 86.5ºC, which was clearly different from the melting temperature of wild-type peaks (87.5ºC; Figure 38C, Figure 38D). To visualize the differences in molecular weight, the RT-qPCR product of one of the replicates of the higher concentration tested for the standard and one replicate of *ΔhaloA* sample were analysed after agarose gel electrophoresis. The result (Figure 39) confirmed that the tested colony was a *H. mediterranei ΔhaloA* knockout mutant since only one amplicon was visible and with a lower molecular weight, when compared to the wild-type amplicon.

Thus, qPCR is valid alterative to discriminate two small sequences (about 100-150 bp) that differ in molecular weight, as different melt peaks are produced.

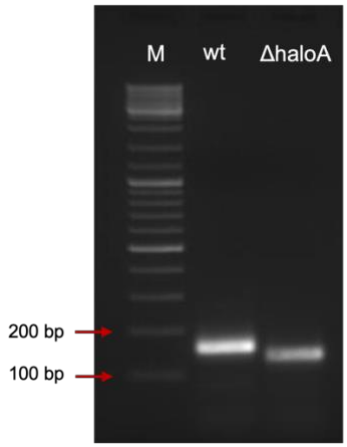

Figure 39. RT-PCR products showing the difference between wild-type and mutant HaloA molecular weight. M corresponds to the GeneRuler DNA Ladder Mix (Thermo Fisher), wt corresponds to the standard.

3.4. Conclusions

During the process of mutants' generation, some problems with the genomic location of *haloA* emerged. The first limitation was the overlap of *haloA* with another gene on the complementary strand of the same genomic region, which allowed the elimination of only 27 bp from *haloA* and restricted the options for primer design to amply its flanking regions. Then, due to the small deleted region, it was not possible to design efficient primers for *haloA* quantification, similarly to what it was done with *ycaO*. Therefore, it was needed to adopt a different strategy to distinguish between pop-out wild-type and pop-out mutants. Even though *H. mediterranei ΔhaloA* took more time to obtain, compared to *H. mediterranei ΔycaO*, the two mutants for haloazolisins' BGC genes were successfully generated and used to perform bioactivity assays, reported in Chapter 4.

The main conclusions of this chapter are:

i) qPCR is more sensitive than Southern blot to validate the absence of any gene copies in mutants;

ii) it is possible to distinguish two fragments of DNA of different size by qPCR thanks to the difference in their melt peaks, and this approach can be successfully used to discriminate between pop-out-mutants and pop-out wild-type.

4. Effect of *ycaO* and *haloA* deletion on the antimicrobial activity of *H. mediterranei*

4.1. Introduction

This study concluded that haloazolisin's *ycaO* and *haloA* genes are transcribed, even at very different rates, in the laboratory conditions used to observe *H. mediterranei* inhibitory activity (Chapter 2). Therefore, to evaluate if such activity is due to the production of these type of RiPPs, *H. mediterranei* knockouts, respectively, for *ycaO* and the *haloA* were successfully generated (Chapter 3) to be tested against other haloarchaea.

As reported in section 1.3.2, the function of YcaO proteins is not exclusively related with the biosynthesis of RiPPs. The best well characterized YcaO in the domain Archaea is probably that of the methanogen *Methanosarcina acetovirans*. This microorganism produces the methyl-coenzyme M reductase (MCR), a key enzyme in methanogenesis that suffers several PTMs, including the thioamidation of a glycine that is catalyzed by an amide-installing YcaO and a TfuA-like protein (Chen, Gan, & Fan, 2020). It was proved that *M. acetovirans* mutant *ΔycaO-tfuA* was not able to synthesize thioglycine because it lacked the main proteins for thiomidation (Nayak, Mahanta, Mitchell, & Metcalf, 2017). Mutant *ΔycaO-tfuA* maintained its viability, showing that genes *ycaO* and *tfuA* are not essential for the producer, but it have lost its thermal stability (Nayak et al., 2017). The YcaO involved in MCR PTMs is an example of a RiPPs-non-related YcaO.

The regulation of RiPP's production is diverse but it normally implies transcriptional regulators and/or other molecules that are often encoded, but not always, in their BGCs. For some RiPPs such as mersacidin, a lanthipeptide produced by *Bacillus* sp. strain HIL Y-85,54728, the presence of the peptide itself is essential for the activation of the regulatory proteins (Schmitz, Hoffmann, Szekat, Rudd, & Bierbaum, 2006). Therefore, deletion of some biosynthetic genes can indirectly impact the transcription of others.

Thus, the objectives of this chapter were to evaluate the transcription level of haloazolisin's genes and the anti-haloarchaea activity of the two mutants generated in Chapter 3 (*H. mediterranei* Δ*ycaO* and Δ*haloA*).

4.2. Materials and Methods

As for Chapter 2, an assay (Figure 40) was outlined to evaluate *H. mediterranei* ⊿*ycaO* and ⊿*haloA* mutants' growth, inhibitory activity and for transcriptional analysis. The number of viable cells and the inhibitory activity of *H. mediterranei* WR510 towards both indicator strains had stabilized after 4 days of growth (section 2.3.1 and 2.3.2). Thus, this was the interval of time chosen to perform the assays presented in this chapter.

Briefly, "dot" plates were prepared by inoculating liquid cultures of the mutants and of *H. mediterranei* WR510 in the centre of YPC-agar plates. The plates were incubated at 37°C for 4 days (96 hours). At day four: i) one plate was used to perform the viable cell counting, ii) one plate was used for RNA extraction and iii) the other two were treated 15 min with UV light and then used to test the mutants' antimicrobial activity against the indicator strains.

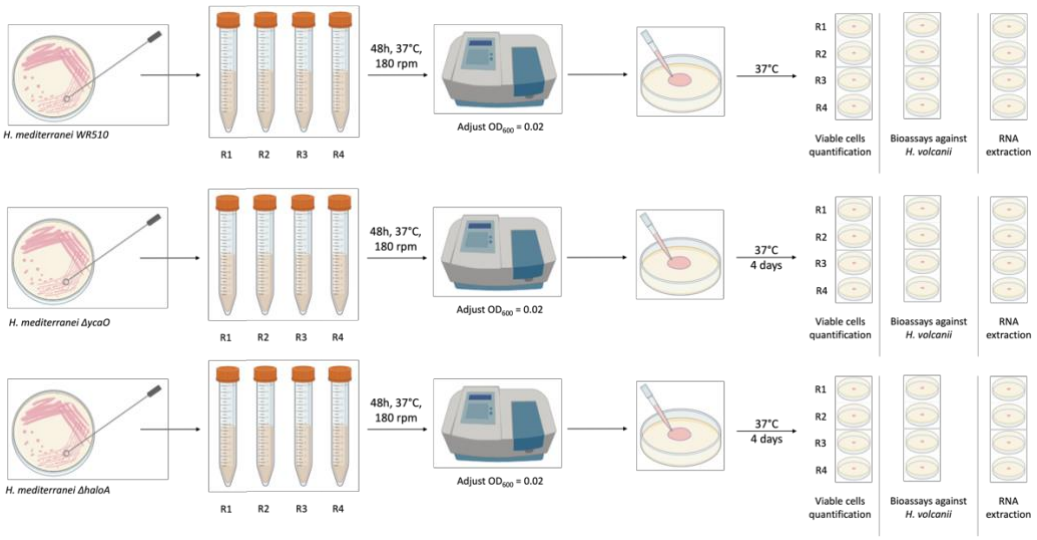

Figure 40. Schematic representation of the assay performed on *H. mediterranei* mutants to evaluate their growth and activity and transcription levels, and to compare them with *H. mediterranei* WR510.

4.2.1. Strains, Medium, and Culture Conditions

H. mediterranei WR510, *H. mediterranei* ⊿*ycaO* and *H. mediterranei* ⊿*haloA* (Table 5) were routinely grown in YPC-agar medium at 37°C for 5 days. *H. volcanii* H33 was cultivated as at section 2.2.1. The plates were stored and conserved at 4°C. All growth media are described in TableS1.

4.2.2. Preparation of cultures and plate inoculation

Plates were prepared as described at section 2.2.2.1 and were incubated at 37°C for 4 days. Four biological replicates were performed (Figure 40).

4.2.3. Viable cells counting

After 4 days, one plate for each biological replicate was used to quantify the number of viable cells in the dot biomass, using an adaptation of the single plate-serial dilution spotting protocol (Thomas et al., 2015), as at section 2.2.2.2.

In the viable cells quantification assay on *H. mediterranei* WR510 (section 2.3.1) resulted that $1x10^{-4}$ was the most appropriated dilution for the CFUs counting. Therefore, only two dilutions, namely $1x10^{-4}$ and $1x10^{-5}$, were plated as in section 2.2.2.2 (Figure 19). The plates were incubated at 37°C for 5 days and, after that, colonies were counted and the number of CFUs/mL determined.

4.2.4. Bioassays against other haloarchaea

At day 4, two plates of each biological replicate were collected and treated for 15 minutes with UV light. Then, the plates were used for overlay bioassay with *H. volcanii*, as described in section 2.2.2.3.

4.2.5. Absolute quantification of gene transcription by qPCR

The expression of *ycaO* and *haloA*, respectively, by *H. mediterranei ΔhaloA* and *ΔycaO,* was determined by absolute quantification via RT-qPCR.

One plate of each biological replicate of *H. mediterranei ΔycaO* and *ΔhaloA* was used for RNA extraction, as reported in section 2.2.3.1. After that, extracted RNA was digested with DNases to eliminate any possibility of DNA contamination and cDNAs of the transcripts were synthesized (section 2.2.3.2). In the end, the cDNAs were used for quantification by RT-qPCR, following the same protocol and parameters reported in section 2.2.2.3.

4.3. Results and Discussion

4.3.1. Viable cell counts

After 4 days of growth, the number of viable cells were respectively 7.42 $x10^7 \pm 2.77x10^6$ CFUs/mL for *H. mediterranei* WR510, 8.15 $x10^7 \pm 1.89$ $x10^7$ CFUs/mL for *ΔycaO*, and $7.32x10^7 \pm 1.39x10^6$ CFUs/mL for *ΔhaloA*.

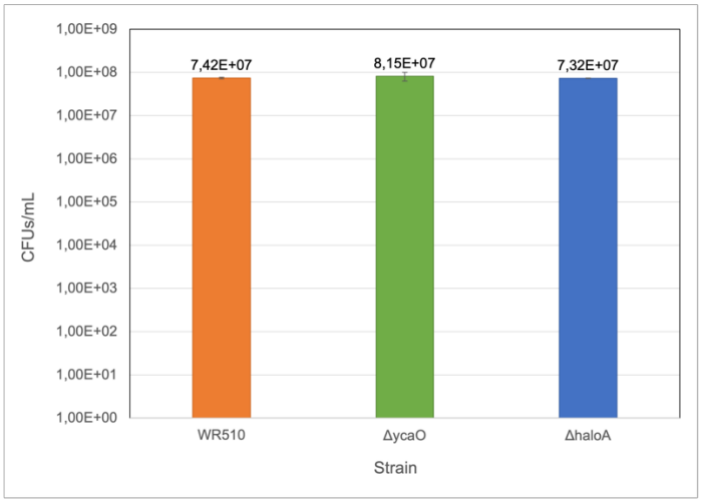

Figure 41. Result of the number of viable cells obtained for *H. mediterranei* WR510, *ΔycaO* and *ΔhaloA* after 4 days of growth in YPC-agar at 37 ºC.

Thus, *H. mediterranei ΔycaO* and *ΔhaloA* strains did not show a significant difference in the number of viable cells when compared with the wild-type *H. mediterranei* WR510 (Figure 41). Also, it is important to highlight that there is no significative difference in the number of CFUs/mL between the two mutants. Therefore, any possible difference in the antihaloarchaea activity of the three strains would not be due to biomass.

4.3.2. Quantification of the transcription levels of *ycaO* and *haloA* genes

In order to verify if the deletion of one gene affected the expression of the other, induced either by genome arrangements or by putative regulation systems, the transcription of *ycaO* and *haloA* by the mutants generated were analysed by RT-qPCR.

As in chapter 2, the analysis of *rpl16* was also included in the analysis and no differences in its quantification were identified between *H. mediterranei* WR510 ($5.97x10^3 \pm 2.30x10^3$ copies/μL), *ΔycaO* ($4.95x10^3 \pm 1.03x10^3$ copies/μL) and *ΔhaloA* ($5.42x10^3$ $\pm 1.41x10^3$ copies/μL).

Quantification of *ycaO* expression in *H. mediterranei* WR510 ($1.74x10^3 \pm 3.01x10^2$ copies/μL) and *ΔhaloA* ($8.87x10^2 \pm 2.22x10^2$ copies/μL) revealed that there is not a significant expression difference among the two strains (Figure 42). These results are similar to the ones obtained in Chapter 2 (section 2.3.3), which confirms the reproducibility of the procedures adopted for the quantification of gene expression in agar media. The same tendency was obtained for the transcription of *haloA* in WR510 ($8.10x10^1$ copies/μL $\pm 2.30x10^1$) and *ΔycaO* ($7.34x10^1$ copies/μL $\pm 1.32x10^1$) strains. Once more, it was confirmed that *haloA* is expressed, but at a low rate (almost 100-fold lower) when compared with *rfl16* or *ycaO*. These data prove that the deletion of one of the two genes (*ycaO* and *haloA*) does not affect the expression of the other; thus, effects observed in the antimicrobial activity (section 4.3.3) will be related with the lack of the gene itself.

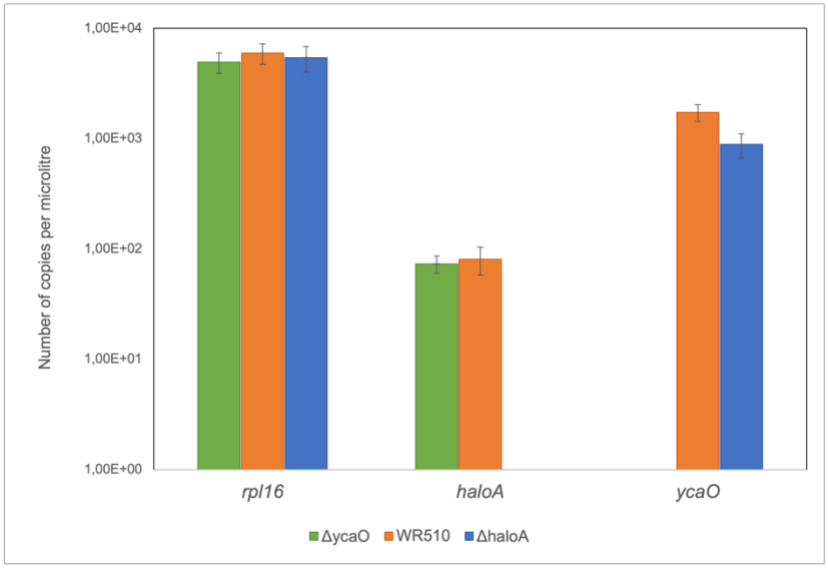

Figure 42. Gene expression quantification of *rpl16*, *haloA* and *ycaO* in strains WR510 *ΔycaO* and *ΔhaloA* after 4 days of growth in YPC-agar.

In the end, as expected, quantification of *haloA* in *H. mediterranei ΔhaloA* and quantification of *ycaO* in *H. mediterranei ΔycaO* was not possible (no amplification was obtained), once more confirming that they are knockout mutants, as already verified at the genomic level in section 3.2.3. Therefore, transcriptional analysis can be used as an alternative, and more sensitive, approach to confirm strains as pop-out (3.2.3.1).

4.3.3. Assessment of anti-haloarchaea activity

Both *H. mediterranei ΔycaO* and *ΔhaloA* retained the inhibitory activity against *H. volcanii* (Figure 43). Still, some differences are noticeable in the halos (Figure 43).

Figure 43. Inhibition halos of *H. mediterranei* WR510, *ΔycaO* and *ΔhaloA* against *H. volcanii* after 4 days of growth.

While the inhibition halo of *H. mediterranei* WR510 against *H. volcanii* measured 40.3 mm (±1.53 mm), the halos of *ΔycaO* and *ΔhaloA* measured, respectively, 47.5 mm (±0.58 mm) and 37 mm (±1.15 mm) (Figure 44). Therefore, after 4 days of growth, the inhibition halo of *H. mediterranei ΔycaO* is, on average, 7 mm bigger compared to that of WR510, and that of *H. mediterranei ΔhaloA* is 3.5 mm smaller in comparison with the wild-type and it is also more diffuse (Figure 43).

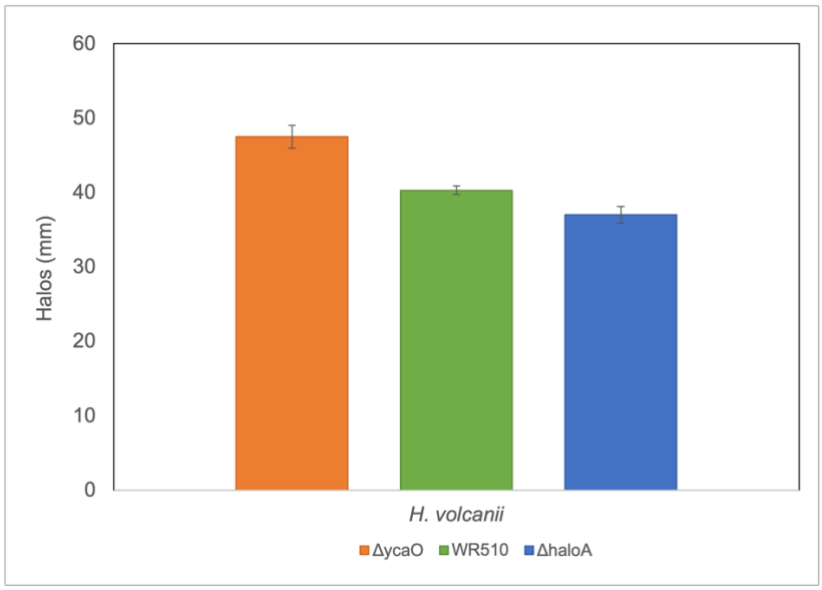

Figure 44. Diameter of the inhibition halos of *H. mediterranei* WR510, *H. mediterranei ΔycaO* and *H. mediterranei ΔhaloA* against *H. volcanii*.

4.4. Conclusions

The main conclusions of this chapter are:

i) The deletion of *ycaO* and *haloA* was also confirmed by transcriptional analysis;

ii) The deletion of *ycaO* and *haloA* genes did not influence the biomass production, when compared with the wild-type strain;

iii) The deletion of *ycaO* or *haloA* does not affect the transcriptional level of *haloA* or *ycaO* genes, respectively;

iv) The mutants retained their anti-haloarchaea activity, which indicates that the haloazolisin BGC is not the main antimicrobial molecule produced by *H. mediterranei* WR510;

v) The absence of modifications installed by YcaO in the cells seem to potentiate the *H. mediterranei* WR510 antihaloarchaea activity.

vi) HaloA seem to contribute slightly to *H. mediterranei* WR510 antihaloarchaea activity and, therefore, might not be a cognate peptide of YcaO;

5. Conclusions and future perspectives

5.1. Conclusions

The main objective of the present work was to verify if *H. mediterranei* antihaloarchaea activity was due to the putative haloazolisin BGC, found in its genome by using bioinformatical tools. The two main constituents of the BGC are gene *haloA*, encoding the precursor peptide, and *ycaO*, encoding a cyclodehydratase, that would be the enzyme responsible for PTM. We generated two *H. mediterranei* mutants, namely *H. mediterranei ΔycaO* and *H. mediterranei Δhalo* and tested them to evaluate: i) the viability of their cells, ii) their transcriptional levels of *ycaO* and *haloA*, and iii) their inhibitory activity. Moreover, assessments of *H. mediterranei* WR510 growth, antimicrobial activity and transcriptional levels were also performed.

The main results were:

- The *H. mediterranei* inhibitory activity reaches its maximum after 4 days in YPC agar;
- In the tested conditions, *haloA* and *ycaO* were expressed in strain WR510, but at very distinct rates;
- In the tested conditions, deletion of *ycaO* and *haloA* did not affect the biomass production;
- The deletion of one of the two genes does not affect the expression of the other, meaning that they do not regulate each other expression;
- HaloA seems to contribute slightly to the antihaloarchaea activity;
- The absence of the PTMs that YcaO catalyses seem to potentiate the antihaloarchaea activity;
- The YcaO of *H. mediterranei* might not be a TOMM-related enzyme;
- HaloA and YcaO (encoded by the essential genes of the putative haloazolisin BGC) are not involved in the biosynthesis of the compounds primarily responsible for *H. mediterranei* antihaloarchaea activity.

Other minor conclusions are:

- The adapted single plate-serial dilution spotting protocol can be used to quantify the number of CFUs in *H. mediterranei*.

5.2. Future perspectives

Since the putative haloazolisin BGC is not the main cause of *H. mediterranei* antihaloarchaea activity, the responsible antimicrobial compounds remain unknown. So, perhaps, the most suitable approach could have been starting from the protein/peptide. The first step would be to separate the supernatant (or agar, if from agar-plate culture) components by HPLC, for example, test their bioactivity and, then proceed to identify the compound responsible for the inhibition by mass spectrometry. Probably the biggest problem for the application of this approach and respective techniques is the high salinity necessary for the antimicrobial compound to retain its activity.

Another aspect that could be the target of further investigations is the YcaO protein. HaloA does not seem to be the cognate peptide of YcaO, and this could be confirmed by performing an *in vitro* reaction containing HaloA, YcaO and ATP. Moreover, a proteomic analysis could be used to understand on which protein/peptide YcaO installs modifications.

5.3. Outputs of this thesis

- iPoster and participation in the World Microbe Forum 2021:
  Cassin E.., Mendo S., Caetano T. Peptides Produced by Halophilic Archaea: Can They Play a Role in Competition?

Bibliography

Ahmed, E., & Holmström, S. J. M. (2014). Siderophores in environmental research: Roles and applications. *Microbial Biotechnology*, 7(3), 196–208. https://doi.org/10.1111/1751-7915.12117

Allers, T., Ngo, H. P., Mevarech, M., & Lloyd, R. G. (2004). Development of Additional Selectable Markers for the Halophilic Archaeon *Haloferax volcanii* Based on the *leuB* and *trpA* Genes. *Applied and Environmental Microbiology*, 70(2), 943–953. https://doi.org/10.1128/AEM.70.2.943-953.2004

Arnison, P. G., Bibb, M. J., Bierbaum, G., Bowers, A. A., Bugni, T. S., Bulaj, G., … van der Donk, W. A. (2013). Ribosomally synthesized and post-translationally modified peptide natural products: overview and recommendations for a universal nomenclature. *Nat. Prod. Rep.*, *30*(1), 108–160. https://doi.org/10.1039/C2NP20085F

Årstøl, E., & Hohmann-Marriott, M. F. (2019). Cyanobacterial siderophores—physiology, structure, biosynthesis, and applications. *Marine Drugs*, 17(5), 281. https://doi.org/10.3390/md17050281

Barry, S. M., & Challis, G. L. (2009). Recent advances in siderophore biosynthesis. *Current Opinion in Chemical Biology*, 13(2), 205–215. https://doi.org/10.1016/j.cbpa.2009.03.008

Besse, A., Peduzzi, J., Rebuffat, S., & Carré-Mlouka, A. (2015). Antimicrobial peptides and proteins in the face of extremes: Lessons from archaeocins. *Biochimie*, Volume 118, 344–355. https://doi.org/10.1016/j.biochi.2015.06.004

Bitan-Banin, G., Ortenberg, R., & Mevarech, M. (2003). Development of a gene knockout system for the halophilic archaeon *Haloferax volcanii* by use of the *pyrE* gene. *Journal of Bacteriology*, *185*(3), 772–778. https://doi.org/10.1128/JB.185.3.772-778.2003

Breil, B. T., Borneman, J., & Triplett, E. W. (1996). A newly discovered gene, *tfuA*, involved in the production of the ribosomally synthesized peptide antibiotic trifolitoxin. *Journal of Bacteriology*, 178(14), 4150–4156. https://doi.org/10.1128/jb.178.14.4150-4156.1996

Burkhart, B. J., Schwalen, C. J., Mann, G., Naismith, J. H., & Mitchell, D. A. (2017). YcaO-Dependent Posttranslational Amide Activation: Biosynthesis, Structure, and Function. *Chemical Reviews*, 117(8), 5389–5456. https://doi.org/10.1021/acs.chemrev.6b00623

Calegari-Santos, R., Diogo, R. A., Fontana, J. D., & Bonfim, T. M. B. (2016). Carotenoid Production by Halophilic Archaea Under Different Culture Conditions. *Current Microbiology*, 72(5), 641–651. https://doi.org/10.1007/s00284-015-0974-8

Castelle, C. J., & Banfield, J. F. (2018). Major New Microbial Groups Expand Diversity and

Alter our Understanding of the Tree of Life. *Cell*, 172(6), 1181–1197. https://doi.org/10.1016/j.cell.2018.02.016

Castro, I. (2019). Halocins and lanthipeptides from *Haloferax mediterranei*.

Chaban, B., Ng, S. Y. M., & Jarrell, K. F. (2006). Archaeal habitats - From the extreme to the ordinary. *Canadian Journal of Microbiology*, 52(2), 73–116. https://doi.org/10.1139/w05-147

Chan, D. C. K., & Burrows, L. L. (2021). Thiopeptides: antibiotics with unique chemical structures and diverse biological activities. *Journal of Antibiotics*, 74, 161–175. https://doi.org/10.1038/s41429-020-00387-x

Chandi, G. K., & Gill, B. S. (2011). Production and characterization of microbial carotenoids as an alternative to synthetic colors: A review. *International Journal of Food Properties*, 14(3), 503–513. https://doi.org/10.1080/10942910903256956

Charlesworth, J. C., & Burns, B. P. (2015). Untapped Resources: Biotechnological Potential of Peptides and Secondary Metabolites in Archaea. *Archaea*, 2015:282035. https://doi.org/10.1155/2015/282035

Chen, H., Gan, Q., & Fan, C. (2020). Methyl-Coenzyme M Reductase and Its Post-translational Modifications. *Frontiers in Microbiology*, 11:578356. https://doi.org/10.3389/fmicb.2020.578356

Cheung, J., Danna, K. J., O'Connor, E. M., Price, L. B., & Shand, R. F. (1997). Isolation, sequence, and expression of the gene encoding halocin H4, a bacteriocin from the halophilic archaeon *Haloferax mediterranei* R4. *Journal of Bacteriology*, *179*(2), 548–551. https://doi.org/10.1128/jb.179.2.548-551.1997

Chibani, C. M., Mahnert, A., Borrel, G., Almeida, A., Werner, A., Brugère, J. F., … Moissl-Eichinger, C. (2020). A comprehensive analysis of the global human gut archaeome from a thousand genome catalogue. *BioRxiv*. https://doi.org/10.1101/2020.11.21.392621

Coker, O. O., Wu, W. K. K., Wong, S. H., Sung, J. J. Y., & Yu, J. (2020). Altered Gut Archaea Composition and Interaction With Bacteria Are Associated With Colorectal Cancer. *Gastroenterology*, 159(4), 1459–1470. https://doi.org/10.1053/j.gastro.2020.06.042

Corcelli, A., Chong, P. L. G., & Koga, Y. (2012). Lipid biology of archaea. *Archaea*, 2012:710836. https://doi.org/10.1155/2012/710836

Costa, H. (2017). Lanthipeptides of Archaea: the case study of *Haloferax mediterranei*. University of Aveiro. Retrieved from http://hdl.handle.net/10773/22043

Cox, C. L., Doroghazi, J. R., & Mitchell, D. A. (2015). The genomic landscape of ribosomal peptides containing thiazole and oxazole heterocycles. *BMC Genomics*, *16*(1), 1–16.

https://doi.org/10.1186/s12864-015-2008-0

Dave, B. P., Anshuman, K., & Hajela, P. (2006). Siderophores of halophilic archaea and their chemical characterization. *Indian Journal of Experimental Biology*, 44(4), 340–344.

Du, Y., Qiu, Y., Meng, X., Feng, J., Tao, J., & Liu, W. (2020). A Heterotrimeric Dehydrogenase Complex Functions with 2 Distinct YcaO Proteins to Install 5 Azole Heterocycles into 35-Membered Sulfomycin Thiopeptides. *Journal of the American Chemical Society*, 142(18), 8454–8463. https://doi.org/10.1021/jacs.0c02329

Dunbar, K. L., Chekan, J. R., Cox, C. L., Burkhart, B. J., Nair, S. K., & Mitchell, D. A. (2014). Discovery of a new ATP-binding motif involved in peptidic azoline biosynthesis. *Nature Chemical Biology*, 10(10), 823–829. https://doi.org/10.1038/nchembio.1608

Dunbar, K. L., & Mitchell, D. A. (2013). Insights into the mechanism of peptide cyclodehydrations achieved through the chemoenzymatic generation of amide derivatives. *Journal of the American Chemical Society*, 135(23), 8692–8701. https://doi.org/10.1021/ja4029507

Ebert, K., Goebel, W., Moritz, A., Rdest, U., & Surek, B. (1986). Genome and gene structures in halobacteria. *Systematic and Applied Microbiology*, 7(1), 30–35. https://doi.org/10.1016/S0723-2020(86)80120-5

Eggersdorfer, M., & Wyss, A. (2018). Carotenoids in human nutrition and health. *Archives of Biochemistry and Biophysics*, Volume 652, 18–26. https://doi.org/10.1016/j.abb.2018.06.001

Eyles, T. H., Vior, N. M., Lacret, R., & Truman, A. W. (2021). Understanding thioamitide biosynthesis using pathway engineering and untargeted metabolomics. *Chemical Science*, 2021: 7138–7150. https://doi.org/10.1039/d0sc06835g

Franz, L., Kazmaier, U., Truman, A. W., & Koehnke, J. (2021). Bottromycins - biosynthesis, synthesis and activity. *Natural Product Reports*, 2021. https://doi.org/10.1039/d0np00097c

Frattaruolo, L., Lacret, R., Cappello, A. R., & Truman, A. W. (2017). A Genomics-Based Approach Identifies a Thioviridamide-Like Compound with Selective Anticancer Activity, 12(11), 2815–2822. *ACS Chemical Biology*. https://doi.org/10.1021/acschembio.7b00677

Fu, X., Liu, R., Sanchez, I., Silva-Sanchez, C., Hepowit, N. L., Cao, S., … Maupin-Furlow, J. (2016). Ubiquitin-like proteasome system represents a eukaryotic-like pathway for targeted proteolysis in archaea. *MBio*, 7(3): e00379-16. https://doi.org/10.1128/mBio.00379-16

Gehring, A. M., Walker, J. E., & Santangelo, T. J. (2016). Transcription regulation in archaea. *Journal of Bacteriology*, *198*(14), 1906–1917. https://doi.org/10.1128/JB.00255-16

Giani, M., & Martínez-Espinosa, R. M. (2020). Carotenoids as a protection mechanism against oxidative stress in *Haloferax mediterranei*, 9(11), 1060. *Antioxidants*. https://doi.org/10.3390/antiox9111060

Giani, M., Miralles-Robledillo, J. M., Peiró, G., Pire, C., & Martínez-Espinosa, R. M. (2020). Deciphering pathways for carotenogenesis in haloarchaea. *Molecules*, 25(5), 1197. https://doi.org/10.3390/molecules25051197

Glick, B. R. (2012). Plant Growth-Promoting Bacteria: Mechanisms and Applications. *Scientifica*, 2012:963401. https://doi.org/10.6064/2012/963401

Gross, E., & Morell, J. L. (1971). The Structure of Nisin. *Journal of the American Chemical Society*, 93(18), 4634–4635. https://doi.org/10.1021/ja00747a073

Gupta, R. S., Naushad, S., Fabros, R., & Adeolu, M. (2016). A phylogenomic reappraisal of family-level divisions within the class Halobacteria: proposal to divide the order Halobacteriales into the families Halobacteriaceae, Haloarculaceae fam. nov., and Halococcaceae fam. nov., and the order Haloferacales into th. *Antonie van Leeuwenhoek, International Journal of General and Molecular Microbiology*, *109*(4), 565–587. https://doi.org/10.1007/s10482-016-0660-2

Han, J., Zhang, F., Hou, J., Liu, X., Li, M., Liu, H., … Xiang, H. (2012). Complete genome sequence of the metabolically versatile halophilic archaeon *Haloferax mediterranei*, a poly(3-hydroxybutyrate-co-3-hydroxyvalerate) producer. *Journal of Bacteriology*, 194(16), 4463–4464. https://doi.org/10.1128/JB.00880-12

Haseltine, C., Hill, T., Montalvo-Rodriguez, R., Kemper, S. K., Shand, R. F., & Blum, P. (2001). Secreted euryarchaeal microhalocins kill hyperthermophilic crenarchaea. *Journal of Bacteriology*, 183(1), 287–291. https://doi.org/10.1128/JB.183.1.287-291.2001

Heider, S. A. E., Peters-Wendisch, P., Wendisch, V. F., Beekwilder, J., & Brautaset, T. (2014). Metabolic engineering for the microbial production of carotenoids and related products with a focus on the rare C50 carotenoids. *Applied Microbiology and Biotechnology*, 98, 4355–4368. https://doi.org/10.1007/s00253-014-5693-8

Henneman, B., van Emmerik, C., van Ingen, H., & Dame, R. T. (2018). Structure and function of archaeal histones. *PLoS Genetics*, *14*(9), 1–21. https://doi.org/10.1371/journal.pgen.1007582

Hider, R. C., & Kong, X. (2010). Chemistry and biology of siderophores, 27, 637–657.

Natural Product Reports. https://doi.org/10.1039/b906679a

Hudson, A. G., Zhang, Z., Tietz, J. I., Mitchell, D. A., & Van der Donk, W. A. (2015). In Vitro Biosynthesis of the Core Scaffold of the Thiopeptide Thiomuracin. *Journal of the American Chemical Society*, *137*(51), 16012–16015. https://doi.org/10.1021/jacs.5b10194

Hwang, S., Chavarria, N. E., Hackley, R. K., Schmid, A. K., & Maupin-Furlow, J. A. (2019). Gene expression of *Haloferax volcanii* on intermediate and abundant sources of fixed nitrogen. *International Journal of Molecular Sciences*, 20(19), 4784. https://doi.org/10.3390/ijms20194784

Igarashi, Y., Kan, Y., Fujii, K., Fujita, T., Harada, K. I., Naoki, H., … Furumai, T. (2001). Goadsporin, a chemical substance which promotes secondary metabolism and morphogenesis in streptomycetes. II. Structure determination. *Journal of Antibiotics*, 54(12), 1036–1044. https://doi.org/10.7164/antibiotics.54.1045

Ireland, C., & Scheuer, P. J. (1980). Ulicyclamide and Ulithiacyclamide, Two New Small Peptides from a Marine Tunicate. *Journal of the American Chemical Society*, 102(17), 5688–5691. https://doi.org/10.1021/ja00537a053

Izawa, M., Kawasaki, T., & Hayakawa, Y. (2013). Cloning and heterologous expression of the thioviridamide biosynthesis gene cluster from streptomyces olivoviridis. *Applied and Environmental Microbiology*, 79(22), 7110–7113. https://doi.org/10.1128/AEM.01978-13

Jones, D. L., & Baxter, B. K. (2017). DNA repair and photoprotection: Mechanisms of overcoming environmental ultraviolet radiation exposure in halophilic archaea. *Frontiers in Microbiology*, 8, 1882. https://doi.org/10.3389/fmicb.2017.01882

Jun, S. H., Reichlen, M. J., Tajiri, M., & Murakami, K. S. (2011). Archaeal RNA polymerase and transcription regulation. *Critical Reviews in Biochemistry and Molecular Biology*, 46(1), 27–40. https://doi.org/10.3109/10409238.2010.538662

Karthikeyan, P., Bhat, S. G., & Chandrasekaran, M. (2013). Halocin SH10 production by an extreme haloarchaeon *Natrinema sp.* BTSH10 isolated from salt pans of South India. *Saudi Journal of Biological Sciences*, 20(2), 205–212. https://doi.org/10.1016/j.sjbs.2013.02.002

Kaur, R., & Tiwari, S. K. (2021). Purification and Characterization of a New Halocin HA4 from *Haloferax larsenii* HA4 Isolated from a Salt Lake. *Probiotics and Antimicrobial Proteins*, 2021 Jul 20. https://doi.org/10.1007/s12602-021-09823-2

Kavitha P. , Lipton A.P., S. A. R. and A. M. S. (2011). Growth Characteristics and Halocin Production by a New Isolate, *Haloferax volcanii* KPS1 from Kovalam Solar Saltern

(India). *Research Journal of Biological Sciences*, *6*(5), 257–262.

Kim, J. Y., Whon, T. W., Lim, M. Y., Kim, Y. B., Kim, N., Kwon, M. S., … Nam, Y. Do. (2020). The human gut archaeome: Identification of diverse haloarchaea in Korean subjects. *Microbiome*, 8(1), 114. https://doi.org/10.1186/s40168-020-00894-x

Klingl, A., Pickl, C., & Flechsler, J. (2019). Archaeal Cell Walls. In *Subcellular Biochemistry*, 92, 471–493. https://doi.org/10.1007/978-3-030-18768-2_14

Koskinen, K., Pausan, M. R., Perras, A. K., Beck, M., Bang, C., Mora, M., … Moissl-Eichinger, C. (2017). First insights into the diverse human archaeome: Specific detection of Archaea in the gastrointestinal tract, lung, and nose and on skin. *MBio*, 8(6):e00824-17. https://doi.org/10.1128/mBio.00824-17

Kumar, V., Saxena, J., & Tiwari, S. K. (2016). Description of a halocin-producing *Haloferax larsenii* HA1 isolated from Pachpadra salt lake in Rajasthan. *Archives of Microbiology*, 198(2), 181–192. https://doi.org/10.1007/s00203-015-1175-3

Kumar, V., & Tiwari, S. K. (2017). Activity-guided separation and characterization of new halocin HA3 from fermented broth of *Haloferax larsenii* HA3. *Extremophiles*, 21(3), 609–621. https://doi.org/10.1007/s00792-017-0930-6

Kumar, V., & Tiwari, S. K. (2019). Halocin Diversity Among Halophilic Archaea and Their Applications. In *Microbial Diversity in Ecosystem Sustainability and Biotechnological Applications*. https://doi.org/10.1007/978-981-13-8315-1_16

Li, Y. M., Milne, J. C., Madison, L. L., Kolter, R., & Walsh, C. T. (1996). From peptide precursors to oxazole and thiazole-containing peptide antibiotics: Microcin B17 synthase. *Science*, 274(5290), 1188–1193. https://doi.org/10.1126/science.274.5290.1188

Li, Y., Xiang, H., Liu, J., Zhou, M., & Tan, H. (2003). Purification and biological characterization of halocin C8, a novel peptide antibiotic from Halobacterium strain AS7092. *Extremophiles*, 7(5), 401–407. https://doi.org/10.1007/s00792-003-0335-6

Liu, H., Han, J., Liu, X., Zhou, J., & Xiang, H. (2011). Development of *pyrF*-based gene knockout systems for genome-wide manipulation of the archaea *Haloferax mediterranei* and *Haloarcula hispanica*. *Journal of Genetics and Genomics*, 38(6), 261–269. https://doi.org/10.1016/j.jgg.2011.05.003

Maksimov, M. O., Pelczer, I., & Link, A. J. (2012). Precursor-centric genome-mining approach for lasso peptide discovery. *Proceedings of the National Academy of Sciences of the United States of America*, 109(38), 15223–15228. https://doi.org/10.1073/pnas.1208978109

Martínez-Espinosa, R. M., Richardson, D. J., Butt, J. N., & Bonete, M. J. (2006). Respiratory

nitrate and nitrite pathway in the denitrifier haloarchaeon *Haloferax mediterranei*. In *Biochemical Society Transactions*, 34(1), 115–117. https://doi.org/10.1042/BST0340115

Martínez-Espinosa, Rosa María, Richardson, D. J., & Bonete, M. J. (2015). Characterisation of chlorate reduction in the haloarchaeon *Haloferax mediterranei*. *Biochimica et Biophysica Acta - General Subjects*, 1850(4), 587–594. https://doi.org/10.1016/j.bbagen.2014.12.011

Matarredona, L., Camacho, M., Zafrilla, B., Bonete, M. J., & Esclapez, J. (2020). The role of stress proteins in haloarchaea and their adaptive response to environmental shifts. *Biomolecules*, 10(10), 1390. https://doi.org/10.3390/biom10101390

Matarredona, L., Camacho, M., Zafrilla, B., Bravo-Barrales, G., Esclapez, J., & Bonete, M. J. (2021). The survival of *Haloferax mediterranei* under stressful conditions. *Microorganisms*, 9(2), 336. https://doi.org/10.3390/microorganisms9020336

Melby, J. O., Nard, N. J., & Mitchell, D. A. (2011). Thiazole/oxazole-modified microcins: Complex natural products from ribosomal templates. *Current Opinion in Chemical Biology*, 15(3), 369–378. https://doi.org/10.1016/j.cbpa.2011.02.027

Meseguer, I., & Rodriguez-Valera, F. (1986). Effect of halocin H4 on cells of *Halobacterium halobium*. *Journal of General Microbiology*, 132(11), 3061–3068. https://doi.org/10.1099/00221287-132-11-3061

Meseguer, Inmaculada, Torreblanca, M., & Konishi, T. (1995). Specific inhibition of the halobacterial Na+/H+ antiporter by halocin H6. *Journal of Biological Chemistry*, 270(12), 6450–6455. https://doi.org/10.1074/jbc.270.12.6450

Mirete, S., Mora-Ruiz, M. R., Lamprecht-Grandío, M., de Figueras, C. G., Rosselló-Móra, R., & González-Pastor, J. E. (2015). Salt resistance genes revealed by functional metagenomics from brines and moderate-salinity rhizosphere within a hypersaline environment. *Frontiers in Microbiology*, 6, 1121. https://doi.org/10.3389/fmicb.2015.01121

Mitchell, D. A., Lee, S. W., Pence, M. A., Markley, A. L., Limm, J. D., Nizet, V., & Dixon, J. E. (2009). Structural and functional dissection of the heterocyclic peptide cytotoxin streptolysin S. *Journal of Biological Chemistry*, 284(19), 13004–13012. https://doi.org/10.1074/jbc.M900802200

Mitra, R., Xu, T., Xiang, H., & Han, J. (2020). Current developments on polyhydroxyalkanoates synthesis by using halophiles as a promising cell factory. *Microbial Cell Factories*, 19, 86. https://doi.org/10.1186/s12934-020-01342-z

Molloy, E. M., Casjens, S. R., Cox, C. L., Maxson, T., Ethridge, N. A., Margos, G., …

Mitchell, D. A. (2015). Identification of the minimal cytolytic unit for streptolysin S and an expansion of the toxin family. *BMC Microbiology*, 15, 141. https://doi.org/10.1186/s12866-015-0464-y

Montalbán-López, M., Scott, T. A., Ramesh, S., Rahman, I. R., van Heel, A. J., Viel, J. H., … van der Donk, W. A. (2020). New developments in RiPP discovery, enzymology and engineering. *Natural Product Reports*, 38(1), 130–239. https://doi.org/10.1039/d0np00027b

Naor, A., Yair, Y., & Gophna, U. (2013). A halocin-H4 mutant *Haloferax mediterranei* strain retains the ability to inhibit growth of other halophilic archaea. *Extremophiles*, *17*(6), 973–979. https://doi.org/10.1007/s00792-013-0579-8

Nayak, D. D., Mahanta, N., Mitchell, D. A., & Metcalf, W. W. (2017). Post-translational thioamidation of methyl-coenzyme M reductase, a key enzyme in methanogenic and methanotrophic archaea. *ELife*, 6:e29218. https://doi.org/10.7554/eLife.29218

Niessen, N., & Soppa, J. (2020). Regulated iron siderophore production of the halophilic archaeon *Haloferax volcanii*. *Biomolecules*, 10(7), 1072. https://doi.org/10.3390/biom10071072

O'Connor, E., & Shand, R. (2002). Halocins and sulfolobicins: The emerging story of archaeal protein and peptide antibiotics. In *Journal of Industrial Microbiology and Biotechnology*, 28(1), 23–31. https://doi.org/10.1038/sj/jim/7000190

Obruca, S., Sedlacek, P., Koller, M., Kucera, D., & Pernicova, I. (2018). Involvement of polyhydroxyalkanoates in stress resistance of microbial cells: Biotechnological consequences and applications. *Biotechnology Advances*, 36(3), 856–870. https://doi.org/10.1016/j.biotechadv.2017.12.006

Oman, T. J., & Van Der Donk, W. A. (2010). Follow the leader: The use of leader peptides to guide natural product biosynthesis. *Nature Chemical Biology*, 6(1), 9–18. https://doi.org/10.1038/nchembio.286

Oren, A. (2008). Microbial life at high salt concentrations: Phylogenetic and metabolic diversity. *Saline Systems*, 4, 2. https://doi.org/10.1186/1746-1448-4-2

Oren, A., & Hallsworth, J. E. (2014). Microbial weeds in hypersaline habitats: The enigma of the weed-like *Haloferax mediterranei*. *FEMS Microbiology Letters*, 359(2), 134–142. https://doi.org/10.1111/1574-6968.12571

Palmer, T., & Berks, B. C. (2012). The twin-arginine translocation (Tat) protein export pathway. *Nature Reviews Microbiology*, 10, 483–496. https://doi.org/10.1038/nrmicro2814

Pašić, L., Velikonja, B. H., & Ulrih, N. P. (2008). Optimization of the culture conditions for

the production of a bacteriocin from halophilic archaeon Sech7a. *Preparative Biochemistry and Biotechnology*, 38(3), 229–245. https://doi.org/10.1080/10826060802164637

Pausan, M. R., Csorba, C., Singer, G., Till, H., Schöpf, V., Santigli, E., … Moissl-Eichinger, C. (2019). Exploring the Archaeome: Detection of Archaeal Signatures in the Human Body. *Frontiers in Microbiology*, 10, 2796. https://doi.org/10.3389/fmicb.2019.02796

Philip, S., Keshavarz, T., & Roy, I. (2007). Polyhydroxyalkanoates: Biodegradable polymers with a range of applications. *Journal of Chemical Technology and Biotechnology*, 82(3), 233–247. https://doi.org/10.1002/jctb.1667

Platas, G., Meseguer, I., & Amils, R. (1996). Optimization of the production of a bacteriocin from Haloferax mediterranei Xia3. *Microbiología (Madrid, Spain)*, 12(1), 75–84.

Platas, Gonzalo, Meseguer, I., & Amils, R. (2002). Purification and biological characterization of halocin H1 from *Haloferax mediterranei* M2a. *International Microbiology*, 5(1), 15–19. https://doi.org/10.1007/s10123-002-0053-4

Poli, A., Di Donato, P., Abbamondi, G. R., & Nicolaus, B. (2011). Synthesis, production, and biotechnological applications of exopolysaccharides and polyhydroxyalkanoates by Archaea. *Archaea*, 2011:693253. https://doi.org/10.1155/2011/693253

Price, L. B., & Shand, R. F. (2000). Halocin S8: A 36-amino-acid microhalocin from the haloarchaeal strain S8a. *Journal of Bacteriology*, 182(17), 4951–4958. https://doi.org/10.1128/JB.182.17.4951-4958.2000

Repka, L. M., Chekan, J. R., Nair, S. K., & Van Der Donk, W. A. (2017). Mechanistic Understanding of Lanthipeptide Biosynthetic Enzymes. *Chemical Reviews*, 117(8), 5457–5520. https://doi.org/10.1021/acs.chemrev.6b00591

Rodrigo-Baños, M., Montero, Z., Torregrosa-Crespo, J., Garbayo, I., Vílchez, C., & Martínez-Espinosa, R. M. (2021). Haloarchaea: A Promising Biosource for Carotenoid Production. In *Advances in Experimental Medicine and Biology*, 1261, 165–174. https://doi.org/10.1007/978-981-15-7360-6_13

Rodriguez-Valera, F., Juez, G., & Kushner, D. J. (1982). Halocins: salt-dependent bacteriocins produced by extremely halophilic rods. *Canadian Journal of Microbiology*, 8(1). https://doi.org/10.1139/m82-019

Rodriguez-Valera, F., Ruiz-Berraquero, F., & Ramos-Cormenzana, A. (1980). Isolation of extremely halophilic bacteria able to grow in defined inorganic media with single carbon sources. *Journal of General Microbiology*, 119(2), 535–538 https://doi.org/10.1099/00221287-119-2-535

Rogers, L. A. (1928). The inhibiting effect of *Streptococcus lactis* on *Lactobacillus*

bulgaricus. *Journal of Bacteriology*, 16(5), 321–325. https://doi.org/10.1128/jb.16.5.321-325.1928

Russell, A. H., & Truman, A. W. (2020). Genome mining strategies for ribosomally synthesised and post-translationally modified peptides. *Computational and Structural Biotechnology Journal*, 18, 1838–1851. https://doi.org/10.1016/j.csbj.2020.06.032

Schalk, I. J., Hannauer, M., & Braud, A. (2011). New roles for bacterial siderophores in metal transport and tolerance. *Environmental Microbiology*, 13(11), 2844–2854. https://doi.org/10.1111/j.1462-2920.2011.02556.x

Schmidt, E. W., Nelson, J. T., Rasko, D. A., Sudek, S., Eisen, J. A., Haygood, M. G., & Ravel, J. (2005). Patellamide A and C biosynthesis by a microcin-like pathway in *Prochloron didemni*, the cyanobacterial symbiont of *Lissoclinum patella*. *Proceedings of the National Academy of Sciences of the United States of America*, 102(20), 7315–7320. https://doi.org/10.1073/pnas.0501424102

Schmitz, S., Hoffmann, A., Szekat, C., Rudd, B., & Bierbaum, G. (2006). The lantibiotic mersacidin is an autoinducing peptide. *Applied and Environmental Microbiology*, 72(11), 7270–7277. https://doi.org/10.1128/AEM.00723-06

Scholz, R., Molohon, K. J., Nachtigall, J., Vater, J., Markley, A. L., Süssmuth, R. D., … Borriss, R. (2011). Plantazolicin, a novel microcin B17/streptolysin S-like natural product from *Bacillus amyloliquefaciens* FZB42. *Journal of Bacteriology*, 193(1), 215–224. https://doi.org/10.1128/JB.00784-10

Shafiee, R. T., Snow, J. T., Zhang, Q., & Rickaby, R. E. M. (2019). Iron requirements and uptake strategies of the globally abundant marine ammonia-oxidising archaeon, *Nitrosopumilus maritimus* SCM1. *ISME Journal*, 13, 2295–2305. https://doi.org/10.1038/s41396-019-0434-8

Shimamura, H., Gouda, H., Nagai, K., Hirose, T., Ichioka, M., Furuya, Y., … Omura, S. (2009). Structure determination and total synthesis of bottromycin A2: A potent antibiotic against MRSA and VRE. *Angewandte Chemie - International Edition*, 48(5), 914–917. https://doi.org/10.1002/anie.200804138

Thomas, P., Sekhar, A. C., Upreti, R., Mujawar, M. M., & Pasha, S. S. (2015). Optimization of single plate-serial dilution spotting (SP-SDS) with sample anchoring as an assured method for bacterial and yeast cfu enumeration and single colony isolation from diverse samples. *Biotechnology Reports*, 8, 45–55. https://doi.org/10.1016/j.btre.2015.08.003

Torreblanca, M., Meseguer, I., & Rodriguez-Valera, F. (1989). Halocin H6, a bacteriocin from *Haloferax gibbonsii*. *Journal of General Microbiology*, 135(10), 2655–2661.

https://doi.org/10.1099/00221287-135-10-2655

Torreblanca, Marina, Meseguer, I., & Ventosa, A. (1994). Production of halocin is a practically universal feature of archaeal halophilic rods. *Letters in Applied Microbiology*, 19(4), 201–205. https://doi.org/10.1111/j.1472-765X.1994.tb00943.x

Torregrosa-Crespo, J., Galiana, C. P., & Martínez-Espinosa, R. M. (2017). Biocompounds from Haloarchaea and Their Uses in Biotechnology. In *Archaea - New Biocatalysts, Novel Pharmaceuticals and Various Biotechnological Applications*. https://doi.org/10.5772/intechopen.69944

Untergasser, A., Cutcutache, I., Koressaar, T., Ye, J., Faircloth, B. C., Remm, M., & Rozen, S. G. (2012). Primer3-new capabilities and interfaces. *Nucleic Acids Research*, *40*(15), 1–12. https://doi.org/10.1093/nar/gks596

Waisvisz, J. M., Van Der Hoeven, M. G., Van Peppen, J., & Zwennis, W. C. M. (1957). Bottromycin. I. A New Sulfur-containing Antibiotic. *Journal of the American Chemical Society*, 79(16), 4520–4521. https://doi.org/10.1021/ja01573a072

Walker, M. C., Eslami, S. M., Hetrick, K. J., Ackenhusen, S. E., Mitchell, D. A., & van der Donk, W. A. (2020). Precursor peptide-targeted mining of more than one hundred thousand genomes expands the lanthipeptide natural product family. *BMC Genomics*, *21*(1), 387. https://doi.org/10.1186/s12864-020-06785-7

Woese, C. R., & Fox, G. E. (1977). Phylogenetic structure of the prokaryotic domain: The primary kingdoms. *Proceedings of the National Academy of Sciences of the United States of America*, 74(11), 5088–5090. https://doi.org/10.1073/pnas.74.11.5088

Woese, C. R., Magrum, L. J., & Fox, G. E. (1978). Archaebacteria. *Journal of Molecular Evolution*, *11*(3), 245–252. https://doi.org/10.1007/BF01734485

Woese, C. R., Magrum, L. J., Fox, G. E., Magrum, L. J., & Balch, W. E. (1978). Classification of methanogenic bacteria by 16S ribosomal RNA characterization. *Proceedings of the National Academy of Sciences of the United States of America*, *74*(10), 4537–4541. https://doi.org/10.1073/pnas.74.10.4537

Woese, Carl R. (1977). A Comment on Methanogenic Bacteria and the Primitive Ecology, *9*, 369–371.

Yorgey, P., Lee, J., Kordel, J., Vivas, E., Warner, P., Jebaratnam, D., & Kolter, R. (1994). Posttranslational modifications in microcin B17 define an additional class of DNA gyrase inhibitor. *Proceedings of the National Academy of Sciences*, *91*(10), 4519–4523. https://doi.org/10.1073/pnas.91.10.4519

Zerulla, K., & Soppa, J. (2014). Polyploidy in haloarchaea: Advantages for growth and survival. *Frontiers in Microbiology*, 5, 274. https://doi.org/10.3389/fmicb.2014.00274

Zuo, Z. Q., Xue, Q., Zhou, J., Zhao, D. H., Han, J., & Xiang, H. (2018). Engineering *Haloferax mediterranei* as an efficient platform for high level production of lycopene. *Frontiers in Microbiology*, 9, 2893. https://doi.org/10.3389/fmicb.2018.02893

Annexes

TableS1. Composition of haloarchaea culture media.

Solution or Medium	Composition (quantities per litre)	Notes
salt-water 30% (SW 30%)	240g NaCl 30g of $MgCl_2 \bullet 6H_2O$ 35g $MgSO_4 \bullet 7H_2O$ 7g of KCl 17.6 mL of a 1M TrisHCl solution (pH 7.5)	After preparation, the solution was autoclaved.
YPC 10X solution	50g of yeast extract (Liofilchem) 10 g peptone of meat (Merck) 10g of casamino acids (Difco Laboratories) 17.6 mL of a 1M KOH solution	After preparation, the solution was autoclaved.
CAM 10X solution	70g of casamino acids (Difco Laboratories) 17.6 mL of a 1M KOH solution	After preparation, the solution was autoclaved.
YPC (yeast-peptone-casamino acids) broth	98 mL of YPC 10X 598 mL of salt-water 30% (SW 30%) 298 mL of distilled water (dH_2O) 6mL of 0.5 M $CaCl_2$	All solutions were prepared and autoclaved separately, and then mixed together in a sterile environment. $CaCl_2$ solution was filter sterilized with a 0.22μm cellulose acetate filter (Frilabo).
YPCss (YPC super salted) broth	98 mL of YPC 10X 896 mL of salt-water 30% (SW 30%) 6mL of 0.5 M $CaCl_2$	All solutions were prepared and autoclaved separately, and then mixed together in a sterile environment. $CaCl_2$ solution was filter sterilized with a 0.22μm cellulose acetate filter (Frilabo).
CAM (casamino acids) broth	98 mL of CAM 10X 598 mL of salt-water 30% (SW 30%) 298 mL of distilled water (dH_2O) 6mL of 0.5 M $CaCl_2$	All solutions were prepared and autoclaved separately, and then mixed together in a sterile environment. $CaCl_2$ solution was filter sterilized with a 0.22μm cellulose acetate filter (Frilabo).
YPC-agar/YPCss-agar/CAM-agar (1.5% agar)	YPC broth/YPCss broth/ CAM broth, 15g of bacteriological agar (Liofilchem)	The corresponding broth was warmed up and 15g of agar per litre were added.
YPC-soft-agar/YPCss-soft-agar (1% agar)	YPC broth/YPCss broth, 10g of bacteriological agar (Liofilchem)	The corresponding broth was warmed up and 10g of agar per litre were added.

TableS2. List of primers.

Target	Primers		Restriction enzyme
	Designation	Sequence (5'→3')	
haloA up region	haloA_UP_FW	CAT**GGATCC**CTCCCTGTATGTACCCCGTC	*Bam*HI
	haloA_UP_RV	TAA**CTCGAG**GCCGTGCCGGAAATCTCC	*Xho*I
haloA down region	haloA_DOWN_FW	TAT**CTCGAG**TCTGAGTCGCTACGCCGT	*Xho*I
	haloA_DOWN_RV	CAT**GGTACC**CGTCGAAGTCTTCCGGAATG	*Kpn*I
ycaO up region	ycaO_UP_FW	GAC**TCTAGA**GGTACTCGGTTCGCTCTCAT	*Xba*I
	ycaO_UP_RV	TAA**GCGGCCGC**GGTCCCCGCAATATCGCC	*Not*I
ycaO down region	ycaO_DOWN_FW	ATT**GCGGCCGC**CAGACGCTGCTCAGACATTC	*Not*I
	ycaO_DOWN_RV	CAT**GGATCC**GGCAACAACCTCATTCCGAA	*Bam*HI
lacZ	pUC19_FW	AGGGTTTTCCCAGTCACGAC	-
	pUC19_RV	CTTCCGGCTCGTATGTTG	-
pyrE	pyrE2_haloferax_FW	CGCAAGAAGGCAAAGGAGTA	-
	pyrE2_haloferax_RV	GACTCCAGTGCGATGTCGT	-
ycaO (qPCR)	check_ycaO_qPCR_Fw	GAGTTGGACGACGCACTCTC	-
	check_ycaO_qPCR_Rv	TGCGACATAGTACGGAAGCG	-
haloA (qPCR)	check_haloA_qPCR_Fw	ATAGTCATCGAGTAGAAGGAAAGCA	-
	check_haloA_qPCR_Rv	ATAGTGACGCTTCGCTTTGGAG	-
haloA	check_UP_haloA	CGGTTCGAACTCCACTTGGA	-
haloA	qPCR_2sdtry_haloA_fw	CGCTACGCCGTCTTTTCCAA	-
	qPCR_2sdtry_haloA_rv	GATGATGAAGAAACGGTGGTC	-
rpl16	qPCR_rpl16s1_F	CCACGTCATCCGCGAGAACA	-
	qPCR_rpl16s1_R	CGACCTTCCCGAACGACTGG	-